STRUCTURAL, METAMORPHIC AND GEOCHEMICAL DISTINCTIONS OF LOW AND HIGH GRADE TERRAINS, FOX MOUNTAIN AREA, NORTH WEST QUEENSLAND

by

PETER W. NASH, B.Sc.

Submitted as partial fulfilment of the
Honours Degree of Bachelor of Science in Geology,
at The University of Adelaide,
November, 1984.

National Grid Reference
SF -54.2 - 6956

TABLE OF CONTENTS

TABLE OF CONTENTS (cont.)

LIST OF FIGURES

LIST OF PLATES

LIST OF TABLES

ABSTRACT

The study area, located in the eastern succession of the Mt. Isa Inlier, consists of interbedded metamorphosed calcareous, pelitic, quartzose and chert sediments of the Mary Kathleen Group.

Two zones with contrasting structural styles and metamorphic grades are present within the study area. An eastern succession of openly crossfolded metasediments and a western tight to isoclinally folded succession intruded by granites of different ages.

Metamorphic grade varies between the two areas. Zone 1, to the east contains mineral assemblages typical of the upper Greenschist Facies while to the west in zone 2, the assemblages typify the Almandine Amphibolite Facies. Garnet-biotite and garnet-hornblende geothermometers indicate temperatures of 430-480°C in zone 1 and temperatures of 600-650°C in zone 2.

Comparison of the two zones, which have been faulted against one another after regional metamorphism, has helped elucidate changes in mineral chemistry and geochemistry with increasing metamorphic grade.

The geochemistry of the two major units; the older Overhang Jaspilite in zone 1 and the overlying Corella Formation in zone 2, show similarities in major element compositions, particularly Al, Ti and Fe, which are related to the source of sediments. Mg, Na and Ca content is generally higher in the Corella Formation and is related to a more evaporitic environment of deposition.

A comparison of dolerites that pervade the study area have been used for the study of changes in mineral chemistry with metamorphic grade, and show changes from tremolite-biotite-albite-epidote assemblages in zone 1 to hornblende-oligoclase/andesine ± garnet assemblages in zone 2.

Garnet-biotite schists of similar bulk rock compositions are found within both zones and show trends from low Ti, high Mg/Mg + Fe in biotite and high CaO + MnO in garnets to high Ti, low Mg/Mg + Fe in biotite and high Fe + Mg in garnets with increasing grade.

I. INTRODUCTION

1.1 Geographical Location

The study area is situated in north-west Queensland on "Chumvale" Cattle Station approximately 20 kilometres west of Cloncurry, as represented by the Marraba Sheet (Reference No. 6956) within the latitudes 20°38' to 20°46' and longitudes 140°16' to 140°25'. Access to the area was via Barkly Highway, central map area, and the Old Mount Isa - Cloncurry Road to the north of the study area. Several subsidiary four wheel drive tracks to waterholes provided access inland from the main roads. Rosebud Orchard, Mary Kathleen, was used as a permanent base.

1.2 Physiography

The topography of the area is primarily controlled by rock lithology. Siliceous breccias and acid igneous bodies form ridges and plateaus. Maximum spot height in the area, at 393 metres above sea level, occurs in the west within outcropping acid igneous bodies.

Ephemeral drainage is controlled by lithology and foliation within the rocks. Strongly foliated metasediments show drainage systems parallel to the foliation trend, while massive quartzose lithologies display radial or meandering drainage patterns.

1.3 Vegetation

Most of the area is vegetated by spinifex with pasture grasses only along water courses. Extensive thickets of acacia shrubs grow preferentially on dolerite outcrops in low lying areas. Stunted eucalypts are present over most of the area, and large river gums border along water courses.

1.4 Climate

The area is characterised by a semi-arid tropical climate with warm dry winter months and monsoonal rainfalls mainly between November and March. Temperature maxima during winter months range from 24° to 32°C with high diurnal range.

1.5 Aims of this Study

The aims of this study are:

(1) to accurately map lithological units within the study area, with emphasis on metamorphism and tectonism;

(2) with the aid of geochemical data, to gain some insight into the changes in rock and mineral chemistry with changes in metamorphic conditions, and

(3) to determine a sequence of structural and metamorphic events.

1.6 Method of Study

The project involved detailed field mapping of the distribution of lithologies and structural trends with the assistance of colour 1 : 20,000 scale photographs obtained from the Bureau of Mineral Resources, and collection of samples for petrological and geochemical studies.

1.7 Previous Studies

Regional mapping in the Mt. Isa - Cloncurry region has been carried out by the Bureau of Mineral Resources and the Geological Survey of Queensland since the early 1960's with the publication of the national 1 : 100 000 B.M.R. sheet series in 1976-77. Carter et. al. (1961) provided the first regional description of the Mt. Isa Inlier and has been followed by Derrick et al. (1971) to provide a review of the regional geological history of the Marraba sheet area. Additional work by Derrick and Wilson (1975), who discussed palaeogeography, stratigraphy, minieralization and tectonics of parts of the area, and more recently Derrick et al. (1976), Glikson et al. (1976), Derrick et al. (1977), Page (1978), Wilson (1978), Blake (1980), and Plumb et al. (1980) provide stratigraphic correlations and discussions of the geological history of the Mt. Isa Inlier. Klemm (1975) provided a detailed map and account of an isolated outcrop of granite in the west of the study area. Mining prospects within the study area indicate there is economic interest in the region, but no data related to this has been published.

The present study is one of three Honours projects undertaken in the Mt.Isa Inlier in 1984 (see Thomas (1984) and Wilson (1984) for further details).

1.8 Regional Setting

The Proterozoic sedimentary sequence and igneous bodies form the North West Queensland Province, which encompasses rocks of possible Lower Proterozoic to Upper Proterozoic age.

The Province extends from the Murphy Tectonic Ridge, in the northwest, which divides it from the McArthur River Basin, to the Mesozoic sediments of the Great Artesian Basin in the east. In the west and south, the Precambrian Province is bordered by Cambrian and Ordovician deposits of the Georgina Basin.

1.9 Stratigraphy

The basement, considered to be the migmatites, gneisses and quartz-mica schists of the Yaringa Metamorphics are suggested to be part of the Tewinga Group of the Mt. Isa Inlier by most authors. This group, consisting of the Leichhardt

Metamorphics, "Magna Lynn Metabasalt", and Argylla Formation outcrop in a median ridge dividing the eastern and western successions. To the west the Leichhardt River Fault Trough (Haslington Group) formed as an unstable basin, while to the east a semistable basin, (Malbon group) and an unstable sloping marine basin formed (Soldiers Cap group). The Malbon Group is disconformable on the Tewinga Group and consists of metabasalt, sandstone, siltstone and minor limestone, with agglomerate and tuff in the western portion of the basin (Marraba Volcanics), which are followed by siltstones, slates, metabasalts and feldspathic quartzites of the Mitakoodi Quartzite. The basalts of the Marraba volcanics show characteristics of continental tholeiites. Basalts in the Soldiers Cap Group (Toole Creek Volcanics) show partly oceanic characteristics, as determined by Wilson (1978). He suggests the presence of a continental margin east of Cloncurry in the Proterozoic and the presence of turbidites in the Soldiers Cap Group to the east, (Glikson 1980) is supportive of this.

Overlying the Marraba Group is the Mary Kathleen Group. The lowest unit in the west of the basin, the Ballara Quartzite, is present where the contemporaneous Overhang Jaspilite is absent. The Overhang Jaspilite forms the basement elsewhere and consists of a calcareous to argillaceous sequence with banded iron formations lying conformably on the Mitakoodi Quartzite.

The overlying Corella Formation consists of a basal calc-silicate granofels unit with limestone and minor quartzite; a psammo-pelitic middle member with calcareous quartzites, basic schists, limestone and calc-silicates; and an upper unit repetitious of the lower Corella unit. Equivalent formations of the Corella; the Marimo Slate, Answer Slate, Stavely and Kuridala Formations represent a period of subsidence and transgression, with the rims of the basin partly submerged (Blake, 1980) resulting in a reduction of sediment supply and the development of restricted basins in which evaporite-carbonate deposits formed.

The final phase of the Middle Proterozoic sedimentation in the eastern basin produced the Deighton, Roxmere and Knapdale quartzites, coinciding with renewed instability in the area with metamorphism accompanied by intrusions of the Wonga Granite, and was followed by widespread gabbroic and granitic plutonism (i.e. Burstall, Tommy Creek, Naraku and Williams Granites, and the Lunch Creek Gabbro).

Deposition of the Quamby Conglomerate is thought to be of Upper Proterozoic age and forms the last unit in the Precambrian sequence of the eastern basin.

II. PETROGRAPHY

The following chapter contains descriptions of the dominant lithologies within the study area. Thin section descriptions are described in Appendix I.

2.1 Mitakoodi Quartzite

The oldest unit occurs in the south of the map area, and also as two isolated domes; one inlier adjacent to Fox Mountain in the north-east and an elongate inlier in the south-east portion of the study area.

The northwards dipping formation is generally low lying except to the far south below metabasalts where the quartzite forms high hogbacks.

The base of the Mitakoodi Quartzite is not present within the study area, but has been reported to conformably overlie the Marraba Volcanics to the south (Derrick et al. 1971). The upper contact appears to be gradational from light phyllitic siltstones of the Mitakoodi Quartzite to dark iron rich siltstones with chert interbeds in the Overhang Jaspilite.

Derrick et al. (1971) recognised three members within the Mitakoodi Quartzite:

1) upper silts and slates;
2) interbedded metabasalt - the 'Wakeful Basalt' member, and
3) feldspathic quartzite.

Silts and slates up to 100m thickness are vertically cleaved with fine bedding still apparent. The unit is light brown, predominantly fine (0.05 to 1.0mm) quartz and muscovite with porphyroblasts of iron oxides.

The metabasalt occurs as a single unit of variable thickness up to 200m conformable with the feldspathic quartzite in the south of the area. The unit consists of massive to cleaved amygdaloidal basalt with quartz filled vesicles. Subophitic textures are preserved with laths of plagioclase (Ab_{98}) contained within a chlorite, biotite, epidote and carbonate groundmass. (Plate 1h.) Directly overlying the basalt are siltstones and schists which coarsen upward into the overlying quartzite.

Pink feldspathic quartzite is the dominant member, with minor inter-bedded siltstones. Sedimentary structures including crossbeds, ripple marks and heavy mineral laminations indicate the member is upright. The majority of the quartzite is medium to coarse grained with variable quantities of quartz and feldspar. Near Fox Mountain very fine grained quartz bands as well as

epidote, feldspar rich layers are present while further east the quartzite contains limonite and magnetite (Plate 2).

2.2 Overhang Jaspilite

The Overhang Jaspilite is the major rock unit in the east of the study area, consisting of predominantly calcareous and silty purple grey metasediments with interbeds of hematitic chert.

The Overhang Jaspilite conformably overlies the Mitakoodi Quartzite. The Overhang Jaspilite and overlying Corella Formation were originally mapped as a single unit by Carter et al. (1961) but was later differentiated by Derrick et al. (1971) on the basis of jaspilite beds within the lower formation. The boundary was taken to be the highest stratigraphic bed containing jaspilite. The thickness of the sequence is difficult to ascertain due to crossfolding. Individual beds attain thicknesses of up to 1.5m but are generally less than 20 cm.

The diversity of rock types within the suite can be grouped broadly on their mineralogy;

1) biotite-scapolite metasiltstones with quartz, orthoclase and calcite. Hand specimens are usually spotted due to poikiloblastic porphyroblasts of scapolite (Me_{54-62}) up to 5mm. Pale brown phlogopite is found with quartz and feldspar in the fine grained matrix (Plate 1a).

2) calcite-tremolite-phlogopite granofels, fine to coarse grained massive calcite with green elongate or fibrous tremolite porphyroblasts up to 6 cm in length (Plate 1d). Calcite content varies from 30 to 80 percent and was probably derived from an impure limestone (Plate 4).

3) biotite-sericite-quartz fine grained argillaceous rock with banding (1 to 10mm) of alternating quartz and micaceous layers, interbedded with calcite, resulting in resistant outcrops between weathered calcite (Plate 3).

4) hematitic chert or jaspilite consisting of cherry red quartzites of variable extent both vertically and laterally. The dominant iron oxides are hematite and magnetite in thin opaque rich and poor layers. Fine quartz grains (0.05 - 0.1mm) are recrystallized and clouded by hematite. Iron free chert bands are common within the unit, resulting in prominent white interbeds between dark calcareous and silty layers.

The boundaries between individual layers are normally abrupt. Sharp contacts indicate rapid variation in depositional environments.

2.3 Chumvale Breccia

The Chumvale Breccia, constituting Fox Mountain and outcrops south of the Barkly Highway, forms upstanding ridges contained within the Overhang Jaspilite, and are closely associated with the Overhang-Mitakoodi Quartzite boundary.

The unit consists of angular blocks and fragments of quartzite up to 2 metres, often with remnant layering of hematitic chert silicified with quartz and brown limonite. The outcrop trends follow the bedding strike within adjacent beds and lie in tightly folded east-west synclines. The breccia has been described by Derrick et al. (1971) as an intraformational tectonic breccia forming as a result of intense folding, brecciation and silicification.

2.4 Corella Formation

Smooth transitions between the Corella Formation and the underlying Overhang Jaspilite are rare within the area, although Derrick et al. (1971) states that the boundary is regionally conformable. Often the boundary is represented by tectonic breccia, fault, or obscured by later sediment deposits.
Rock types within the area can be separated into the Lower and Middle Corella members (Derrick et al. (1971)).

2.4.1 Lower Corella Member

The Lower Member is a medium to coarse grained, red, coarsely bedded calc-silicate granofels. Plagioclase, microcline, diopside and hornblende are the main constituents within a matrix of calcite, quartz and minor epidote. The granofels are interbedded with finely laminated shales and siltstones, and isolated pods of coarse pebbly quartzite occur. The outcrop of the Lower Corella member attains a thickness of 250 metres and is conformably overlain by the more pelitic units of the Middle Corella member.

2.4.2 Middle Corella Member

This unit includes interbedded limestone, metasiltstone, pelitic schist, basic schist, calc-biotite granofels and calc-silicate granofels. No stratigraphic order is inferred.

2.4.2.1 Biotite and muscovite schist

Predominantly muscovite and biotite (0.5 - 1.2mm) and fine grained quartz and feldspar. Colour varies from black to grey brown, and is well foliated and often crenulated. The foliation is defined by layers of aligned mica laths and elongate recrystallized quartz lenses. In some schists almandine garnet is abundant as porphyroblasts up to 2cm and the schists tend to be more

mafic in composition. The garnets are usually poikiloblastic with biotite, muscovite, quartz, calcite and feldspars crystallized in the pressure shadows around the garnets.

2.4.2.2 Calc-biotite granofels

The granofels consist of medium to coarse grained calcite, biotite and rare almandine garnet and encompass a range of lithologies between light coloured pelitic or psammitic schists and granofels.

2.4.2.3 Calc-silicate granofels

Characterised by coarse calcite and fine to coarse quartz and feldspar with biotite and/or hornblende coexisting with tremolite and epidote. (Plates 1b, 1c). Banding has developed by metamorphic differentiation parallel to the original bedding resulting in monomineralic amphibole and feldspar bands up to 15mm thick (Plate 5).

2.4.2.4 Limestone and marl

Within metapelites and calc-silicates thin grey laterally discontinuous limestone beds are present. Calcite is coarsely crystalline with no internal sedimentary structure. Uncontaminated calcite pods are massive and highly fractured and may be fault related.

2.4.2.5 Metapelites, metapsammites and quartzites

Fine grained thin beds of pelitic and psammitic composition are inter-calated with graphitic layers of sedimentary origin. Thick quartzites with little or no calcite are ridge forming and show strong lineations.

2.5 Calc-silicate breccia

This intraformational breccia (Derrick et al. (1971)) is contained within the Corella Formation and outcrops as isolated hills and boulders to the north and south-east. It contains clasts of lithologies similar to those of surrounding areas, including chert fragments, laminated siltstones, fine grained red quartzites and calc-silicate granofels. The matrix consists of tremolite, calcite, plagioclase and quartz. Clast sizes vary from minute to several metres (Plate 6).

2.6 Metadolerites

Dolerites of various thickness pervade most lithologies within the area and are concordant to subconcordant with the original bedding. The dolerites show subophitic textures with laths of plagioclase in a tremolite, chlorite, epidote, biotite groundmass. Grainsizes range from fine at igneous-sedimentary contacts to coarsely crystalline in the centres of large intrusions (Plate 1g).

2.7 Amphibolites

The amphibolites, up to 70 metres thick, are contained within the Corella Formation and are generally concordant with the stratigraphy. Where folding is intense, laterally extensive bands of metasediments have been incorporated in the amphibolites, and where there are discordant relationships to metasediments the amphibolites are of obvious intrusive origin. Assemblages of coarse blue green hornblende, plagioclase, ilmenite and minor quartz is ubiquitos (Plate 1e, 1f). Pale pink almandine garnet is well developed near the edges of the sills.

2.8 Tommy Creek Microgranite

The granite is located along the upper western boundary of the map area forming rugged hills and plateaus, and is surrounded by Corella schists and calc-silicates, which the granite intruded concordantly. The outcrop patterns are related to cross folding within this area, and because of this, the true thickness of the granite is difficult to determine.

The granite is fairly homogeneous mineralogically with quartz, plagioclase, microcline, biotite and rare calcite. Porphyroblasts of quartz and plagioclase are common, the groundmass shows a gneissic and locally mylonitic texture (Plate 7).

2.9 Naraku Granite

Only isolated intrusions of this coarse grained leucocratic rock occur within the region, but they are part of a massive intrusion located north-east of the area. The granite has approximately equal amounts of quartz and feldspars and small quantities of muscovite.

2.10 Rhyolite

One minor outcrop of rhyolite occurs within the Tommy Creek Microgranite and consists of plagioclase phenocrysts within a fine matrix of quartz, plagioclase and hornblende. The groundmass is undeformed and the foliation present is the result of magmatic flow around the phenocrysts.

2.11 Depositional Environment

The stratigraphy represented in the area consists of a fining upward sequence of marine origin. The Mitakoodi Quartzite is feldspathic and contains ripple marks and crossbeds indicating a near shore environment close to the sediment source. Gradual fining upwards marks the boundary to the Overhang Jaspilite and the development of a low energy restricted environment indicated by the presence of finely bedded carbonates and jaspilite beds. Cl rich scapolites in metasiltstones suggest evaporitic conditions with high initial salt content in the rocks (Ramsay et al. 1970).

PLATE 1

a : poikiloblastic porphyroblasts of scapolite with randomly orientated subhedral biotite and anhedral epidote 830/24
(x 32 plane light)

b : subhedral tremolite and plagioclase with kink twinned calcite 830/65
(x 125 plane light)

c : tremolite porphyroblasts in sericitised plagioclase and minor zoisite 830/96
(x 32 cross polars)

d : fibrous radiating actinolite in a matrix of calcite and iron oxides (dark) 830/I.2
(x 32 cross polars)

e : fractured porphyroblasts of garnet with twinned interstitial calcite, subhedral hornblende and clinozoisite 830/151
(x 32 plane light)

f : garnet porphyroblasts with hornblende defining an S_1 foliation, minor clinozoisite in a sericitised plagioclase groundmass
(x 32 cross polars) 830/151

g : plagioclase laths with intergrown hornblende altering to biotite 830/63
(x 125 plane light)

h : euhedral epidote crystal surrounding ilmenite and intergrown with anhedral biotite and plagioclase 830/35
(x 125 plane light)

Plate 1

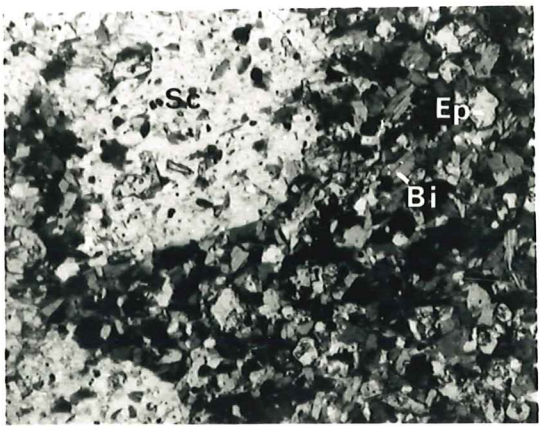

a

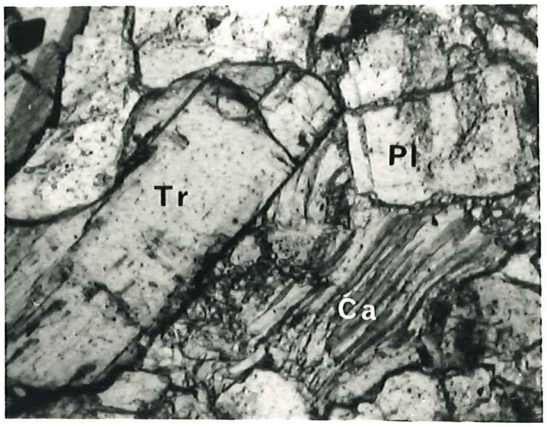

b

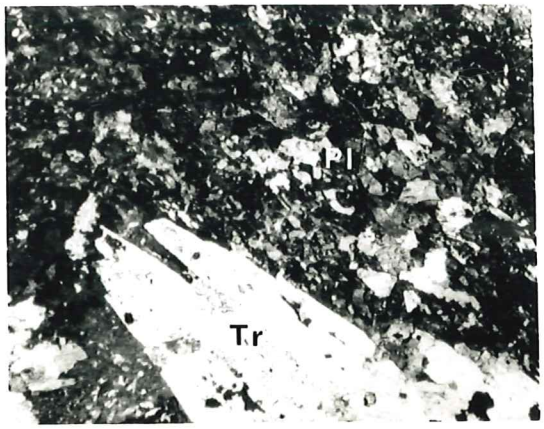

c

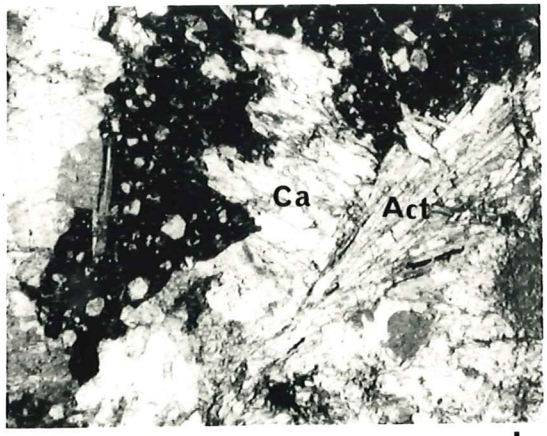

d

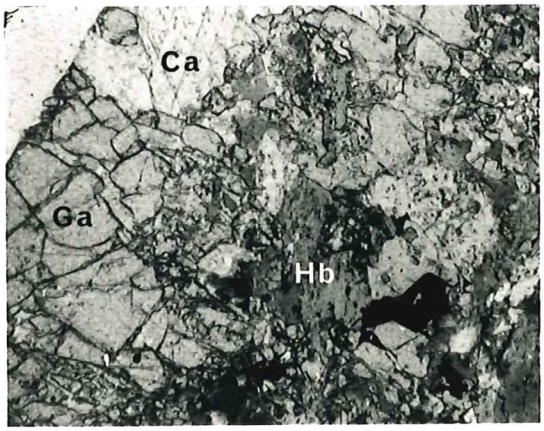

e

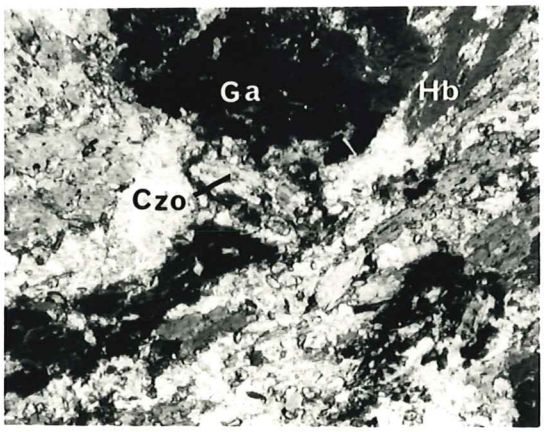

f

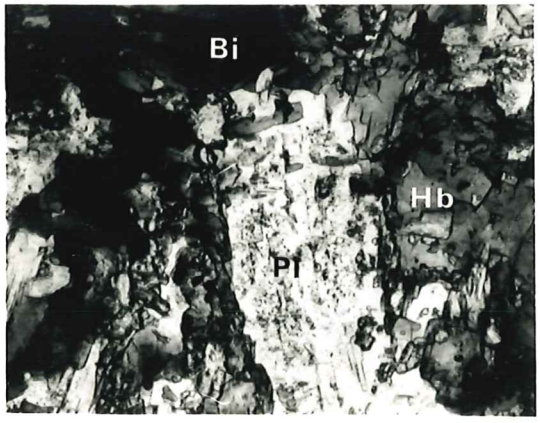

g

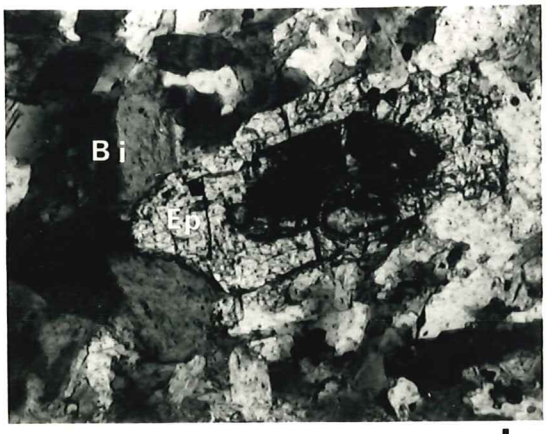

h

Plate 2

Mitakoodi Quartzite-the spotted appearance is due to leaching of iron oxide pods.

Plate 3

Interbedded chert, marl and finely bedded siltstone within the Overhang Jaspilite.

Plate 4

Overhang Jaspilite with red jaspilitic beds (right) in close association with calcareous beds (left). The dark spotting in the limestone represents porphyroblast of actinolite.

2

3

4

Plate 5

Banding within the Corella formation as the result of metamorphic differentiation. Bands of pink feldspar are clouded by find hematitic "dust" and are interbedded with dark amphibole rich layers.

Plate 6

Corella Breccia with large blocks up to 50 cm.

Plate 7

Tommy Creek Microgranite with strong lineations indicating intense deformation related to D_1.

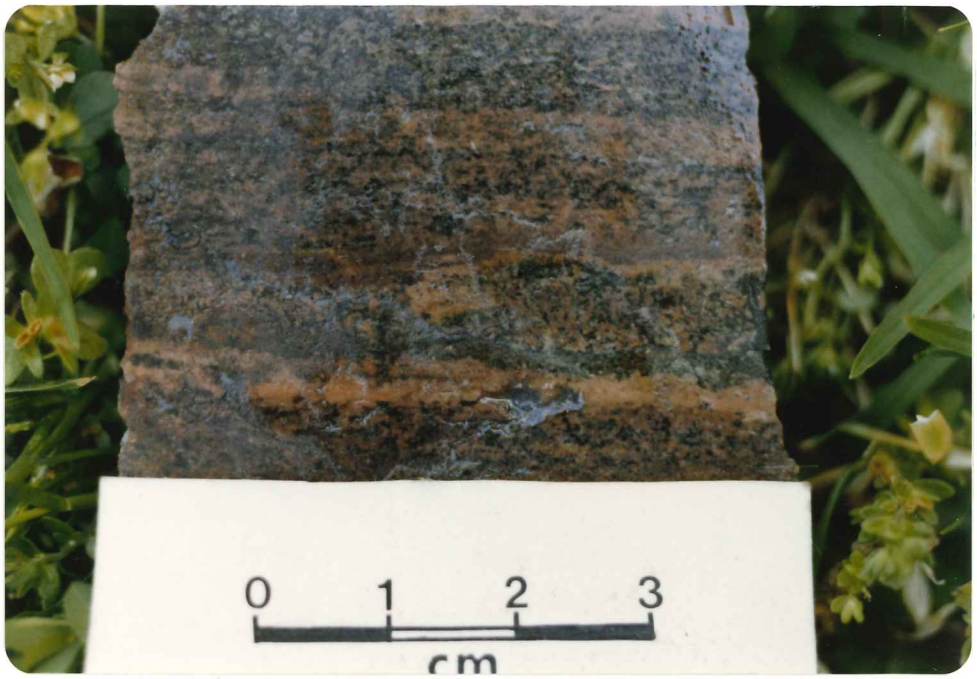

5

6

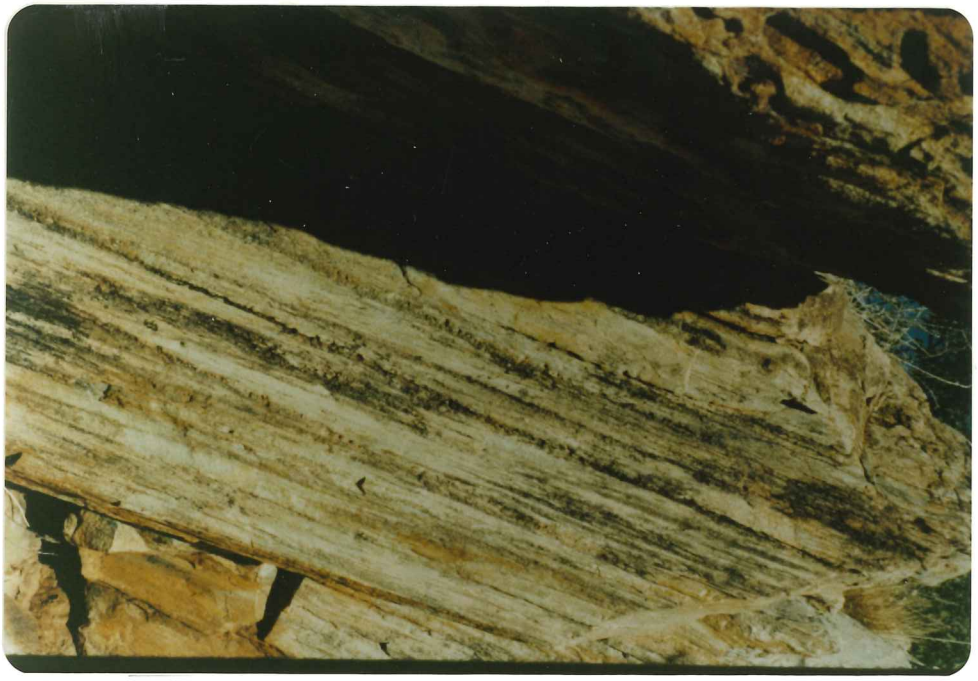

7

III. STRUCTURAL INTERPRETATION

The following chapter discusses structural geology within the study area. A geological map and interpretive cross-section of the study area may be found in the back pocket of this thesis.

3.1 Structural Setting

The study area is situated at the closure of the Duck Creek Anticline which plunges in a north-easterly direction and runs parallel to the Bulonga Anticline to the west. A north-west trending fold system has resulted in cross-folding, and the development of inliers of Mitakoodi Quartzite within the Overhang Jaspilite.

3.2 Structural Zones

The study area can be separated into two zones based on the fold intensities:

(1) to the east and south, open to tightly cross folded metasediments are folded about a north east trending anticline.

(2) to the north west, tight to isoclinal, cross folded, strongly folitated and metamorphically banded metasediments and acid igneous rocks form narrow synclines and anticlines of variable orientations.

Zone 1

To the east and south of the area, two major folding events can be seen. An early north-west tightly folded system (F_1) and a later north-east trending open fold system (F_2) plunging 30-40° towards 40°. The first folding event is best developed in the Overhang Jaspilite near the Mitakoodi Quartzite contact, where the Chumvale Breccia is present in tight elongate synclines, though F_1 is not observed in the Mitakoodi quartzite (Figure 2c).

The second deformation event is persistent throughout the area and has resulted in the rotation of F_1 fold axes around the Duck Creek Anticline and the development of a persistent cleavage throughout the area. Resultant structures are basin and dome crossfolds such as Fox Mountain in the north-east, exposing Mitakoodi Quartzite within the surrounding Overhang Jaspilite.

Zone 2

In the north-west of the study area, the Corella Formation is folded into tight to isoclinal, locally overturned synclines and anticlines of variable orientations. The dominant directions are north-east, north-west and east trending systems resulting from complex crossfolding. Crenulation relationships suggest the north-west S_1 foliation predates the north-east S_2 foliation.

Rotation of north-west fold axes to a more easterly direction is the result of F_2 folding.

Folding events within the area are related. F_1 within the north-west has resulted in strong axial planar foliation. Metamorphic differentiation parallel to the foliation and bedding in calcareous rocks is a product of isoclinal folding in this region. To the east F_1 is present as open to tight anticlines and synclines with only a weak penetrating foliation. Fold limbs steepen in close proximity to the Chumvale Breccia which has been suggested by Derrick (1971) to be an intraformational breccia.

The north-east trending system (F_2) is persistent throughout the study area and varies only in deformation intensity. To the south and east, the F_2 folds in the Mitakoodi Quartzite are open while to the north-west steeply dipping crossfolded S_1 foliations show that tight folding associated with S_2 is prevalent.

3.3 Faulting

A number of large vertical faults exist within the area and generally strike north-south.

Within the Corella Formation, faulting parallel to the S_1 foliation is ductile, developing zones of intense shearing which is difficult to distinguish from the foliation. Microstructures in quartzites near the fault trending north within the Corella shows mylonitic textures (Plate 8c).

Faulting to the south of the Butcher Creek - Barkly Highway crossing shows a more brittle style of faulting with brecciation confined to a narrow band and has little effect on surrounding lithologies.

The contact between the Overhang Jaspilite and the Corella formation appears to be faulted in most cases. The orientation of the faulting is difficult to ascertain but displacement must be large because of the changes in structural intensity and metamorphic grade on either side of the fault.

3.4 Interference Structures

Interference structures resulting from the two deformations are variable and are dependent on the orientations of F_1 and F_2.

To the east in the vicinity of Fox Mountain, symmetrical basin and dome structures are the result of F_1 fold axes being near perpendicular to F_2. Further

east and south-east more elongate structures formed where the two fold axes intersect at angle much less than 90°.

To the north-west, the cross folding is more complex, as shown by the outcrop patterns. Similarities of outcrop patterns with patterns described by Ramsay (1967) indicates that the one fold axis (F_1) is not upright resulting in "mushroom" interference structures.

Figure 2

Stereographic projections of bedding and foliations within the study area

Fig.2

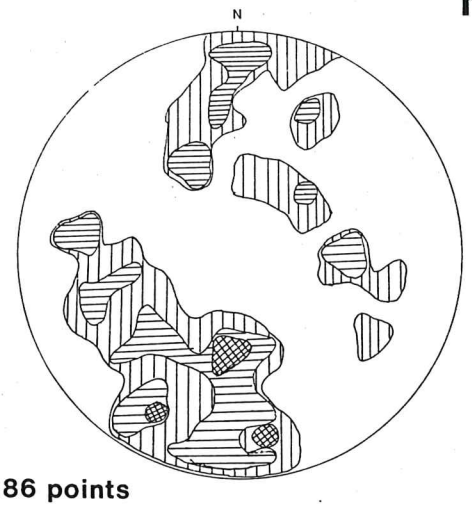

186 points

POLES OF BEDDING IN OVERHANG JASPILITE (SOUTH OF BARKLY HIGHWAY)

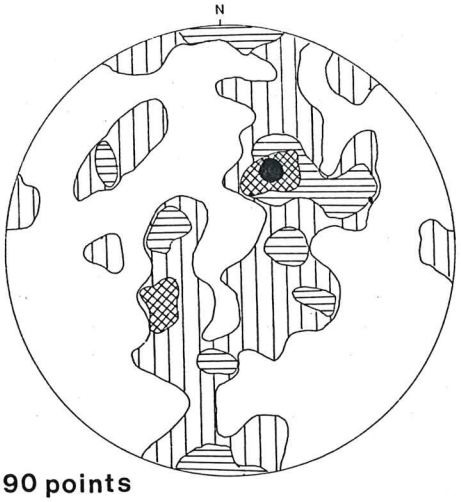

90 points

POLES OF BEDDING IN OVERHANG JASPILITE (FOX MOUNTAIN AREA)

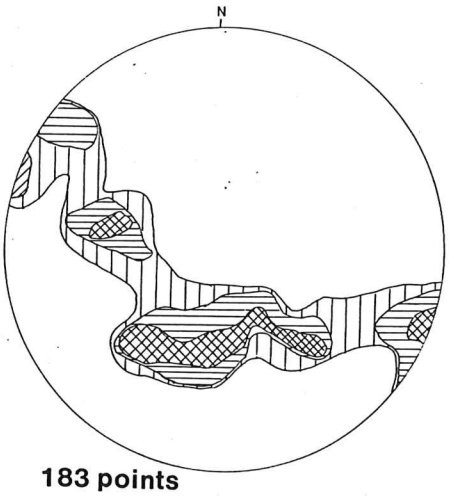

183 points

POLES OF BEDDING IN MITAKOODI QUARTZITE

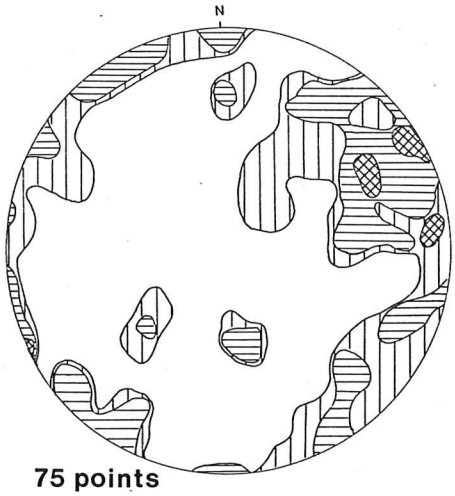

75 points

POLES OF FOLIATION IN CORELLA SCHISTS AND CALC-SILICATES

IV. METAMORPHISM

4.1 Polymetamorphism

Three metamorphic events can be distinguished in the study area. Contact metamorphism related to the emplacement of the Tommy Creek Microgranite before regional metamorphism (M_1) cannot be distinguished as a separate metamorphic event due to overprinting by the later M_1. Regional metamorphism affected the whole area and resulted in the development of mineral assemblages stable in the upper Greenschist Facies of metamorphism in zone 1 and in the Amphibolite Facies in zone 2. The second metamorphic event, M_2, is related to the emplacement of the Naraku Granite. Small contact aureoles containing high grade mineral assemblages, particularly an increased abundance of diopside in calc-silicates and garnet regrowths in biotite schists characterise this event.

The isolated occurrence of mineral growth associated with the granite intrusion may be related to subsurface minor plutons heating rocks within the immediate vicinity of the granite.

The third metamoprhic event is of minor occurrence and represents retrograde metamorphism with the breakdown of amphibole to biotite, garnet to chlorite, K feldspar to talc (Klemm, 1975), clouding of plagioclase with hematite due to leaching of iron from ferromagnesium minerals, and Ca rich plagioclase altering to albite, with excess Ca being incorporated into epidote (Winkler, 1979).

4.2 Metamorphic-Deformational History

The emplacement of the Tommy Creek Microgranite has been dated by Page (1982) at 1600 Ma. The timing of metamorphism appears to be a two stage event; one at 1620-1670 Ma and a younger event at ~ 1500 Ma (Page, 1983b). Both metamorphic events post date the deposition of the Corella Formation, and due to the fact that contact metamorphism has been overprinted by regional metamorphism around the microgranite, the youngest metamorphic event is suggested to coincide with the regional metamorphism within the study area.

The S_1 foliation within the area is defined by minerals formed during prograde metamorphism. This feature alone is not sufficient to suggest M_1 relates to D_1 in zone 2 because isoclinal folding will cause even randomly orientated minerals to become subparallel by mechanical rotation. Inclusion trails in poikiloblastic garnets and K feldspars in pelitic schists are parallel to the S_1 foliation, suggesting syntectonic growth or possibly rotation. Evidence from some garnet porphyroblasts in schists suggest that D_1 is post M_1, due to the fact that S_1 foliations wrap around fractured garnets (Plate 9).

Within zone 1 a similar relationship of D_1 and M_1 can be seen. D_1 crenulations of M_1 metamorphic banding occur only outside scapolite porphyroblasts formed during prograde metamorphism (Plate 11). Subhedral biotite flakes have grown parallel to the D_1 fold axes suggesting minor thermal activity during D_1 and probably represents the waning stages of regional metamorphism (Plate 12).

The second metamorphic event can be related to the north-east D_2 folding event. Crenulations of the S_1 foliation by F_2 in garnet biotite schists in zone 2 is preserved in garnet rims (Plate 8a). Rotation during growth of K feldspar porphyroblasts with the rims orientated parallel to S_2 suggests pre- and syntectonic growth (Plate 8b). The source of renewed thermal activity is suggested to be the intrusion of the Naraku granite, and with the development of north-south foliations in the granite, the intrusion has been suggested to be in the waning stages of this tectonothermal event (Derrick, et al. 1971).

The changes in orientation of inclusion in garnets coinciding with S_1 and S_2 is gradual, indicating the changes in orientations of stress fields are gradual or closely related in time.

4.3 Metamorphic Facies

The zones of regional metamorphic grade are defined on the basis of mineral assemblages and mineral compositions. Basic and pelitic rocks are useful in defining metamorphic grade while calc-silicates tend to have varied compositions and mineralogies.

Two broad zones can be defined, and are shown in Figure 3:

Zone 1: Weakly metamorphosed sediments with original sedimentary textures preserved. They are generally fine grained and consist of metasiltstones, slates, limestones, marls and quartzites. Dolerites show preserved subophitic textures but pyroxenes have been altered to amphiboles. The diagnostic assemblage quartz-albite-epidote indicates this zone belongs to the Greenschist Facies defined by Turner (1960). Rocks of pelitic composition contain biotite-muscovite-chlorite-sphene ± albite ± epidote mineral assemblages. Basic rocks commonly contain actinolite-epidote-albite-chlorite-sphene ± quartz ± biotite assemblages typical of the Quartz-Albite-Epidote-Biotite Subfacies of Turner (1960). With the presence of almandine in suitable rock types the Quartz-Albite-Epidote-Almandine Subfacies is indicated, but with restricted occurrence.

Zone 2: Rock types are generally coarser grained with stronger schistose fabric with the loss of fine bedding features. Gross bedding features are enhanced by metamorphic differentiation parallel to the bedding. Diagnostic

mineral assemblages hornblende -plagioclase-almandine and hornblende-plagioclase-epidote in basic rocks and the assemblages quartz-almandine-muscovite-biotite-plagioclase ± epidote in pelitic schists coincide with the Almandine Amphibolite Facies of Turner (1960).

4.4 Mineral Assemblages

Metamorphic assemblages with rock units are as follows.

Zone 1

Pelitic rocks

830/24 quartz-orthoclase-epidote-scapolite-biotite-chlorite-muscovite

830/8 quartz-microcline-albite-scapolite-phlogopite-chlorite-calcite

Calcareous rocks

830/I.2 tremolite-biotite-calcite-iron oxide

830/I.3 quartz-albite-orthoclase-scapolite-biotite-calcite

Basic rocks

830/1 tremolite-plagioclase-epidote-chlorite-ilmenite

830/21 tremolite-plagioclase-chlorite-muscovite-clinozoisite-ilmenite-sphene

Zone 2

Pelitic rocks

830/52 quartz-microcline-garnet-biotite-muscovite

830/88 quartz-microcline-muscovite-graphite

Calcareous rocks

830/65 actinolite-plagioclase-calcite

830/105 hornblende-plagioclase-microcline-diopside-chlorite-epidote-zoisite

Basic rocks

830/84 hornblende-calcite-clinozoisite-sericite-ilmenite

830/151 quartz-hornblende-garnet-clinozoisite-sericite-ilmenite

4.5 Mineral Reactions

Within zone 1 Ca amphiboles may form by the following reactions

chlorite + calcite + quartz → actinolite + H_2O + CO_2

dolomite + quartz + H_2O → tremolite + calcite + CO_2

Phlogopite forms by reactions involving dolomite

3 dolomite + K feldspar + H_2O → phlogopite + 3 calcite + $3CO_2$

2 quartz + 3 dolomite + muscovite → phlogopite + 2 calcite + $4CO_2$ + anorthite

In the absence of dolomite, as in pelitic rocks, the following reaction is likely

muscovite + chlorite → biotite + chlorite

Almandine may form at slightly higher grades in place of Fe bearing chlorite by the reactions

chlorite + quartz → garnet + H_2O

chlorite + biotite$_{(1)}$ + quartz → garnet + biotite$_{(2)}$ + H_2O

Within zone 2 the presence of hornblende, oligoclase/andesine in basic rocks suggests the following reactions may be occurring

Ca amphiboles → hornblende

epidote + chlorite → actinolite + anorthite + H_2O

or albite + zoisite → oligoclase

Diopside formation is usually the result of the reaction

tremolite + calcite + quartz → diopside + CO_2 + H_2O

4.6 Conditions of Metamorphism

4.6.1 Introduction

In the following chapter, consideration of the conditions of metamorphism will be discussed. The main considerations will be the determination of temperatures, pressures and fluid compositions.

4.6.2 Geothermometry

With changes in temperature, mineral assemblages may exchange ions firstly between sites in two different minerals (intercrystalline exchange) or secondly, between different sites in one mineral (intracrystalline exchange).

4.6.3 Garnet-Biotite Geothermometer

The exchange reaction:-

$K\,Mg_3Si_3AlO_{10}(OH)_2 + Fe_3Al_2Si_3O_{12} = K\,Fe_3Si_3AlO_{10}(OH)_2 + Mg_3Al_2Si_3O_{12}$

phlogopite almandine annite pyrope

is an intercrystalline exchange of Fe and Mg that varies with temperature.

Five different geothermometers for garnet-biotite pairs were applied using a computer program developed by Fanning (1980). Results are shown in Table 1. The method of Ferry and Spear (1978) is the only geothermometer that takes into account the dependence of K_D (see Appendix V) on pressure and temperature. Values can be extrapolated to the desired pressure.

Three of the methods are in general agreement (Ferry and Spear (1978), Perchuck (1976) and Thompson (1976)). The method of Saxena (1969) produces lower temperature values, and the Two Parameters temperatures of Goldmann and Albee (1977) give much higher results.

For zone 1 garnet-biotite pairs, values vary from 431°C to 483°C for the Ferry and Spear method. The value of Saxena (1969) is as low as 344°C which is too low for the metamorphic facies involved. Zone 2 shows a range of values from 541°C to 684°C at 3kb. The wide range of values is expected because of the superimposing of different metamorphic events. Garnet rims growing during M_2 provide similar temperatures to garnet cores growing during M_1.

4.6.4 Garnet-hornblende Geothermometer

The intercrystalline exchange of Fe and Mg between garnet and hornblende may be represented by the exchange reaction

$$\underset{\text{ferro-pargasite}}{\tfrac{1}{4}\,NaCa_2Fe_4Al_3Si_6O_{22}(OH)_2} + \underset{\text{pyrope}}{\tfrac{1}{3}\,Mg_3Al_2Si_3O_{12}} = \underset{\text{pargasite}}{\tfrac{1}{4}\,NaCa_2Mg_4Al_3Si_6O_{22}(OH)_2} + \underset{\text{almandine}}{\tfrac{1}{3}\,Fe_3Al_2Si_3O_{12}}$$

Graham and Powell (1984) calibrated this reaction against a garnet-clinopyroxene geothermometer using data on coexisting garnet-hornblende-clinopyroxene assemblages and obtained good correlation between garnet-hornblende and garnet-clinopyroxene temperatures. Values obtained for almandine garnet-hornblende pairs are in the range of 650°C, which is comparable to the values obtained from garnet-biotite pairs.

4.6.5 Hornblende Geothermometry

Experimental work on hornblendes by Spear (1981) resulted in the determination of the variations in elemental proportions within the hornblende structure with temperature, pressure and oxygen fugacity. Correlation of hornblendes within the study area and those of Spear's show a temperature range of 610°C to 660°C for amphibolites in zone 2 and temperatures of 550°C for metadolerites of zone 1 (Figure 4a).

This method is only qualitative due to the fact that experimental data is derived from rocks of tholeiitic composition with very low K content, which may deviate greatly from the starting compositions of rocks within the study area.

4.6.6 Geobarometry

The lack of critical mineral assemblages within the study area does not allow for the accurate determination of pressure conditions. The presence of garnet-clinozoisite hornblende assemblages in amphibolites is indicative of high pressures suited to the Albite Epidote Amphibolite Facies. For almandine garnet to form in common rock types above 500°C, pressures must exceed 4 Kbars (Winkler, 1979). Clinozoisite is stable at high pressures, particularly high fluid pressures exceeding 4 Kbars (Winkler, 1979).

Correlations with the experimental data on hornblendes by Spear (1981) gave pressure estimates of between 1.5 and 4.5 Kbars (Figure 4b). Na, Ti, Mn and Al^{iv} proportions in hornblendes give pressure estimates of between 1.5 and 3 Kbars while Fe/Fe + Mg, Mg, Fe total and Si give pressure estimates of between 1.5 and 4 Kbars. The wide variation in values is the result of varied original compositions of the rocks, affecting the elemental proportions in hornblende.

4.6.7 Fluid compositions

Fluid pressures and fluid compositions are as equally important in determining mineral assemblages within the area as temperature and pressure.

The range of rock types within the area suggests fluid compositions would be highly variable. Ferry (1976) indicated that during metamorphism, large X_{CO2} gradients exist from bed to bed scale in interbedded limestones, calc-silicates and pelites. Decarbonation reactions producing diopside and tremolite in calcareous beds would result in initially high X_{CO2} in metamorphic fluids. Pelitic rocks undergo dewatering reactions during prograde metamorphism, resulting in high X_{H2O} within metamorphic fluids. Interbedded calcareous and pelitic units implies large X_{H2O}/X_{CO2} ratios of fluids between beds (Thompson, 1976), and fluctuations in pressure conditions would be expected between beds of differing compositions if total pressure (P_{total}) does not equal $p_{H2O} + p_{CO2}$.

4.6.8 Determination of Fluid Compositions

Within amphibolites of zone 2, interstitial calcite and hornblendes incorporating chlorine suggest that Ca and Cl may be significant components within migrating fluids. The assemblage calcite-quartz-orthoclase-biotite-garnet-hornblende within one thin section of amphibolite (sample 830/57) allows the determination of partial pressures of H_2O and CO_2 from the reactions

1 anorthite + quartz + 2 calcite = grossularite + $2CO_2$ (1)

and

5 phlogopite + 6 calcite + 24 quartz =

= 3 tremolite + 5 orthoclase + $6CO_2$ + $2H_2O$ (2)

Using microprobe and experimental thermodynamic data, calculation of f_{CO2} and f_{H2O} by the method of Ferry (1976b) (Appendix V) provided a CO_2 fugacity (f_{CO2}) of 1390 bars at T = 773°K and P_{total} = 3500 bars for reaction (1). Substitution of the derived f_{CO2} into reaction (2) at the same T and P provides f_{H2O} = 1103 bars. In terms of partial pressures p_{CO2} = 525 bars and p_{H2O} = 3127 bars. The sum of the fluid pressures approximates, within experimental error, the assumed pressure of 3500 bars, which indicates that other fluid components did not contribute significantly to the total pressure. The results also suggest that $P_{total} = p_{H2O} + p_{CO2} = P_{fluid}$, which is in agreement with Ferry (1976b).

The formation of oligoclase (An_{16-32}) in the amphibolites requires moderately high p_{CO2}, while the presence of clinozoisite indicates very low p_{CO2} (Winkler, 1979). Fluctuations in fluid compositions is likely to have caused the variation, with plagioclase forming during periods of high p_{CO2} and clinozoisite forming during periods of high p_{H2O}.

Within calc-silicates p_{CO2} is expected to be higher than that determined for the amphibolites due to the decarbonation reaction (4) given below

muscovite + calcite + 2 quartz = microcline + anorthite + CO_2 + H_2O (3)

and

tremolite + 3 calcite + 2 quartz = diopside + $3CO_2$ + H_2O (4)

The assemblage tremolite-diopside-muscovite-calcite-quartz-plagioclase-microcline-zoisite (sample 830/105) allows the determination of p_{CO2} using the above reactions. Assuming p = 3500 bars and T = 823°K, then p_{CO2} = 314 bars and the mole fraction of CO_2 (X_{CO2}) = 0.09. If $P_{total} = p_{CO2} + p_{H2O}$ then $p_{H2O} \approx$ 3153 bars. The very low p_{CO2} may not be indicative of CO_2 content during regional metamorphism, because reaction (4) indicates high p_{CO2} should develop relative to p_{H2O}. The problem could be solved if lower temperatures were postulated for the formation of diopside. Figure 5 shows that at lower temperatures, X_{CO2} for reaction (4) decreases.

The presence of zoisite and plagioclases of different compositions in the assemblage suggests the reaction:

3 calcic plagioclase + calcite + H_2O = 2 zoisite + intermediate plagioclase + CO_2 (5)

where the intermediate plagioclase is more Na enriched than the calcic plagioclase. The reaction can be driven to the right by high p_{H2O}, and on Figure 5 the reaction requires lower X_{CO2} than reaction (4). The high H_2O can be attributed to either the influx of H_2O rich fluids released from the dehydration

reactions in neighbouring pelitic rocks during regional metamorphism, or from admixtures of H_2O-rich magmatic fluids (Ferry, 1978). The close association of this particular unit to the Tommy Creek Microgranite, and the absence of pelitic lithologies close by, suggests the source of the fluid could be from the granites. Dating of the granites by Page (1978) indicates the granite predate the regional metamorphism, so that the development of a zoisite-two plagioclase assemblage is not the result of contact metamorphism. Zoisite in the calc-silicates, as opposed to clinozoisite in amphibolites does not appear to be the product of prograde metamorphism, as it is not integrown with prograde minerals such as diopside or microcline. The suggestion that zoisite is a product of retrograde metamorphism is probable, particularly when the temperature of equilibrium for reaction (5), derived from thermodynamic data and calculations by Ferry (1976b) is lower at 426°C than regional metamorphism.

Not all calc-silicates contain zoisite and many contain high proportions of calcite, suggesting that X_{CO2} may be higher in some calc-silicates.
Fluctuations will vary according to rock chemistry and the abundance of water.

Within zone 1, the accurate determination of fluid composition is hampered by the lack of suitable mineral assemblage. Most reactions at a low grade of metamorphism are dehydration reactions, releasing water. High p_{H2O} values are expected, although the formation of tremolite in calcareous rocks is a decarbonation reaction:-

dolomite + quartz + H_2O → tremolite + calcite + CO_2 (6)

resulting in high CO_2 pressures.

4.6.10 Summary - Conditions of Metamorphism

From the above discussion, the features of metamorphism are as follows:-

1) Temperatures and pressures of prograde metamorphism in zone 2 reached values of 600 to 650°C and 3-4 Kbars respectively.
Similar temperatures were attained during contact metamorphism.
In zone 1, temperatures of 430-480°C and similar pressures to zone 2 were attained (see Figure 6).

(2) Fluid compositions are postulated to be highly variable between beds and with time. pCO_2 has been reduced during prograde metamorphism in amphibolites to allow clinozoisite to form. High pCO_2 in calc-silicates has been lowered to allow the formation of zoisite during retrograde metamorphism.

Plate 8a

Garnet porphyroblast rims overgrowing F_2 crenulations. Cores are orientated parallel to S_1 830/52 (x 32 plane light)

Plate 8b

K feldspar showing pre- and syntectonic growth and rotation, with rims parallel to S_2 830/52 (x 32 plane light)

Plate 8c

Development of mylonitic textures in quartzite with grainsize reduction and quartz lenses parallel to S_1 830/168 (x 32 plane light)

Plate 8d

Kinked twins in plagioclase and the development of foliation around the porphyroblast 830/46 (x 32 cross polars)

Plate 9

Development of S_1 foliation around garnet and quartz porphyroblasts. Scale in cm.

Plate 8

a

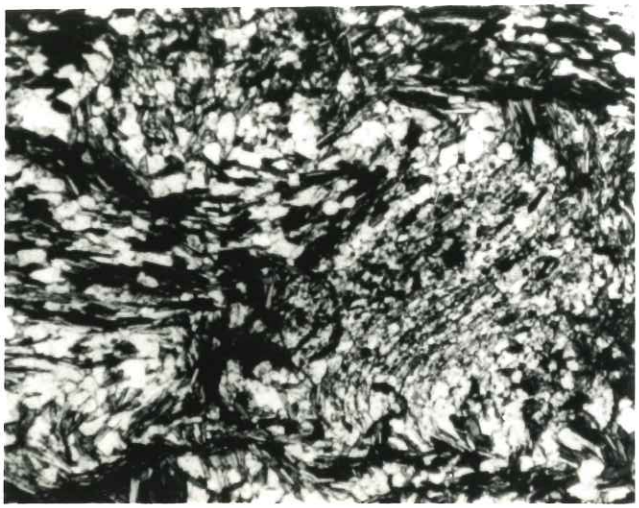

b

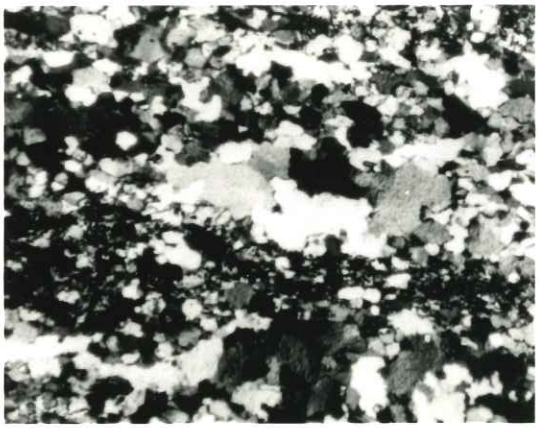

c

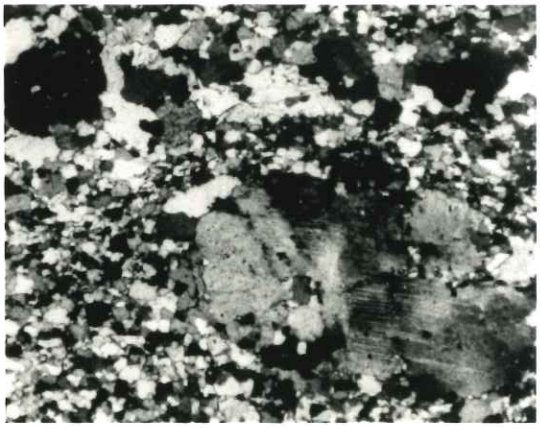

d

Plate 9

Plate 10

Development of S_1 foliation perpendicular to bedding in garnet biotite schist, zone 1 830/81 (x 32 plane light)

Plate 11

Porphyroblasts of scapolite in metasiltstone with crenulated laminations in matrix only 830/30 (x 32 plane light)

Plate 12

Development of biotite in metasiltstone parallel to F_1 830/30 (x 125 plane light)

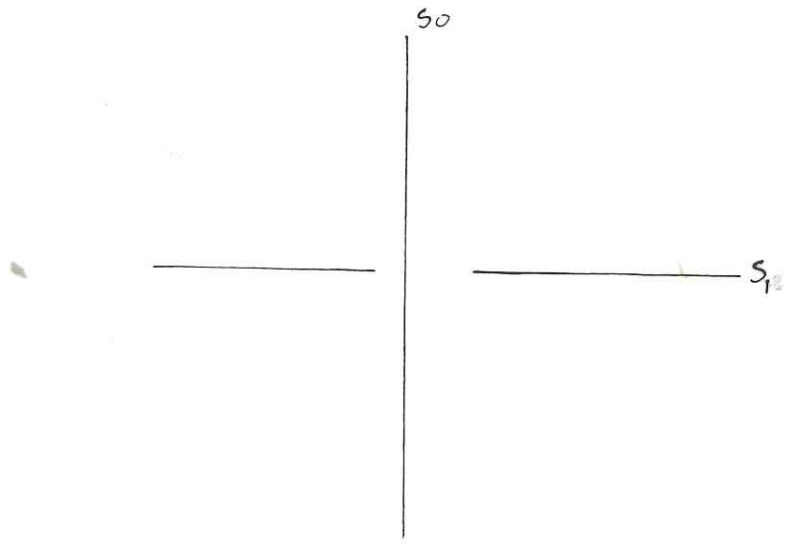
S_0
S_1

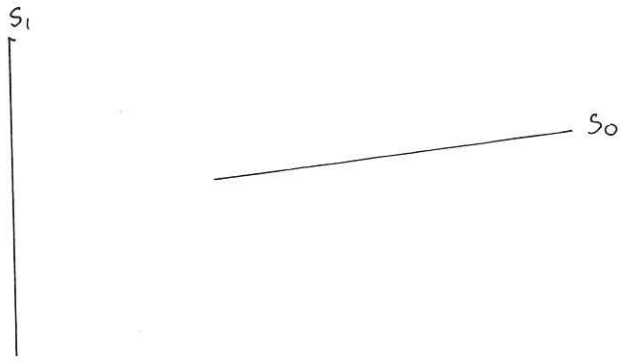
S_1
S_0

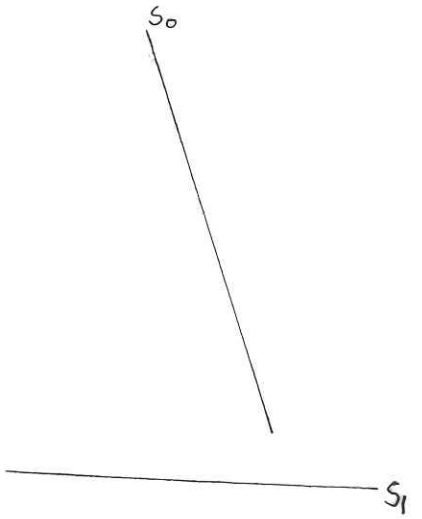
S_0
S_1

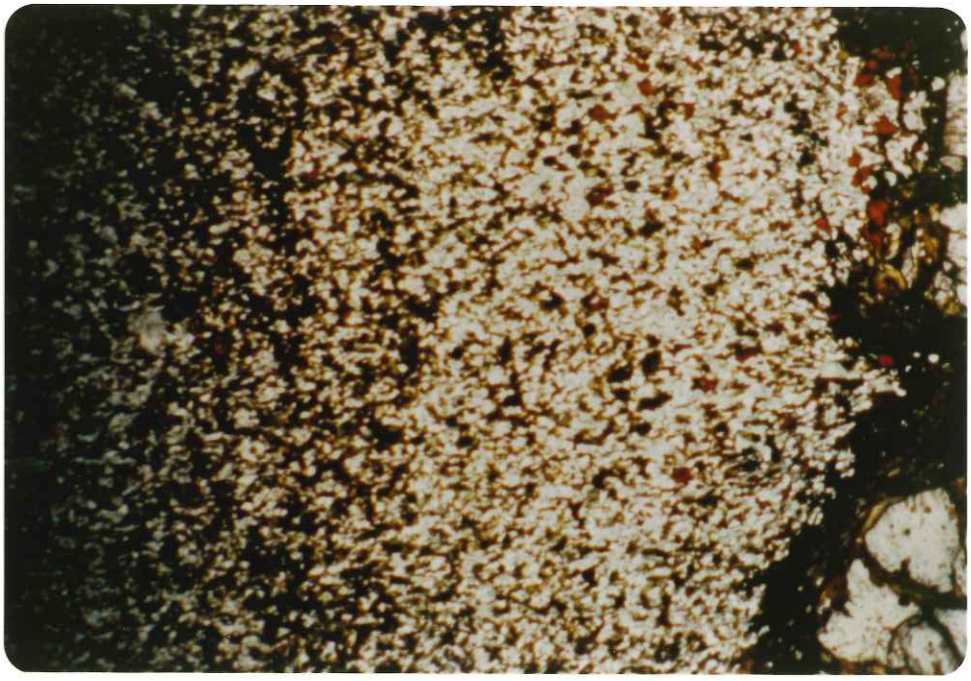

10

11

12

Figure 3

Metamorphic zones of the study area according to mineral assemblages

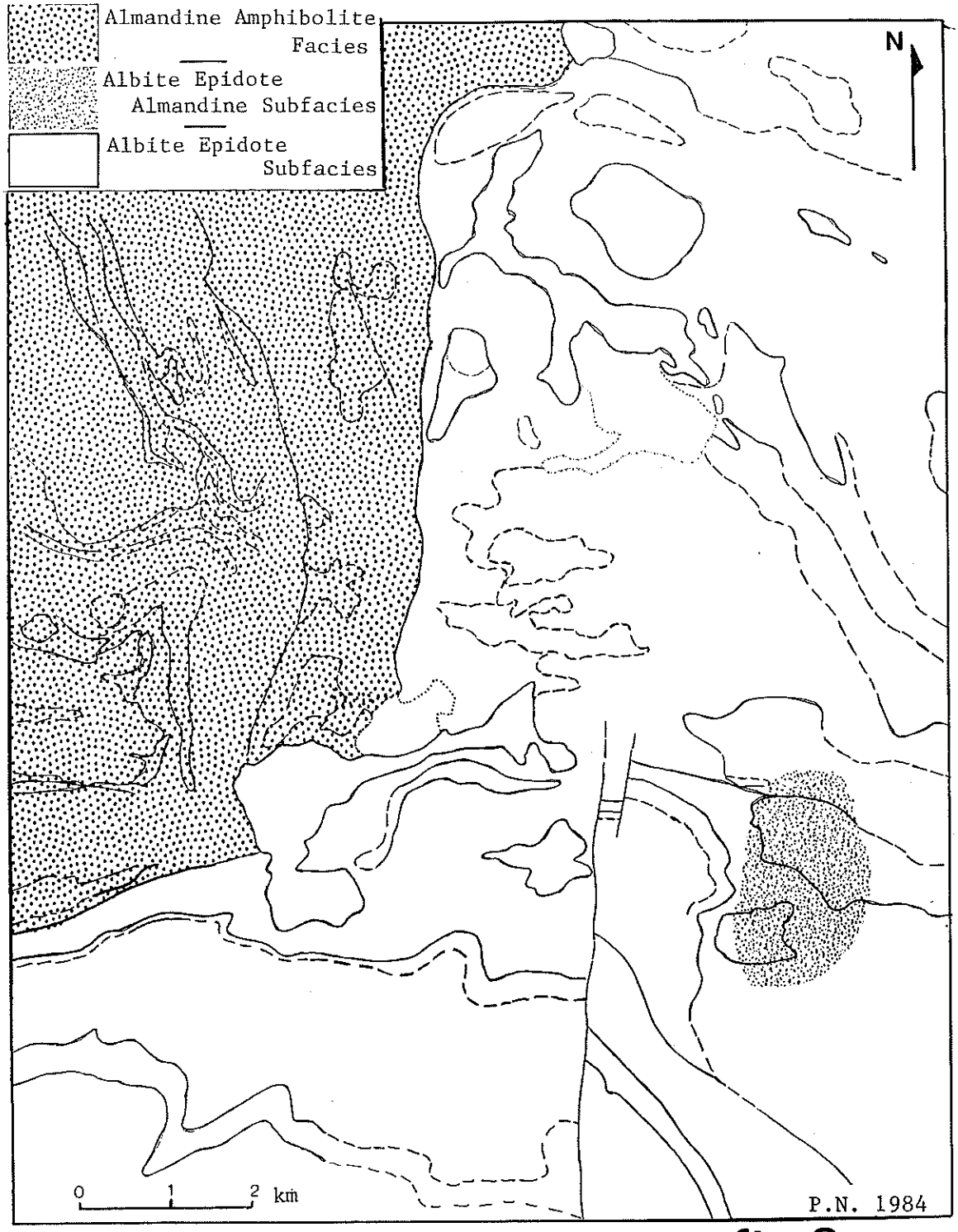
Almandine Amphibolite Facies
Albite Epidote Almandine Subfacies
Albite Epidote Subfacies
N
0
1
2 km
P.N. 1984

fig. 3

Table 1

Temperature determinations using Garnet-Biotite Geothermometers

(temperatures in °C)

Figure 4a

Cation proportions of amphiboles in the study area against temperature of formation in °C (after Spear, 1981)

Figure 4b

Cation proportions of amphiboles in the study area against $P_{fluid} = P_{total}$ in Kbars (after Spear, 1981)

	Garnet-Biotite pair	Ferry and Spear (1978) (3kb)	Perchuck (1976)	Thompson (1976)	Saxena (1969)	Goldmann & Albee (1977)
Zone 1	830/81 P_1	431	488	456	320	599
	P_2	483	522	493	344	622
Zone 2	52 rim	704	650	695	447	719
	core	692	643	658	530	713
	57 P_1	541	559	540	493	649
	111 P_1	643	617	625	454	693
	P_2	684	640	650	440	709
	119 P_1	671	632	644	442	705
	P_2	614	601	598	407	681

Table 1 : Garnet-Biotite Geothermometer

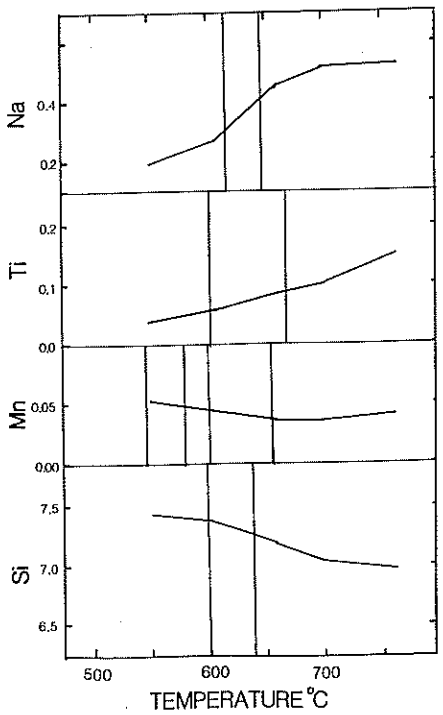

fig. 4a

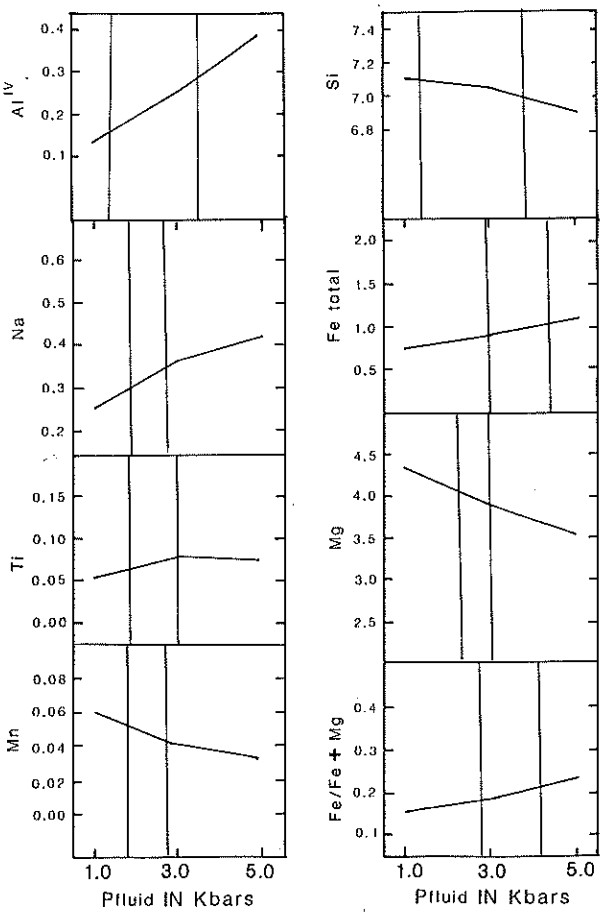

fig. 4b

Figure 5

T-X(H_2O - CO_2) diagram for some equilbria in the CaO - K AlO_2 - MgO -Al_2O_3 - SiO_2 - CO_2 - H_2O system at $P_{total} = P_{H2O} + P_{CO2}$ = 5 Kbar (after Thompson, 1975).

Abbreviations

Anr : anorthite
Cal : calcite
Czo : clinozoisite
Dio : diopside
Mic : microcline
Mus : muscovite
Tre : tremolite
Qtz : quartz

Figure 6

P T conditions for regional metamorphism in comparison to phase relations of the Greenschist – Amphibolite transition boundary (after Maruyama,]983)

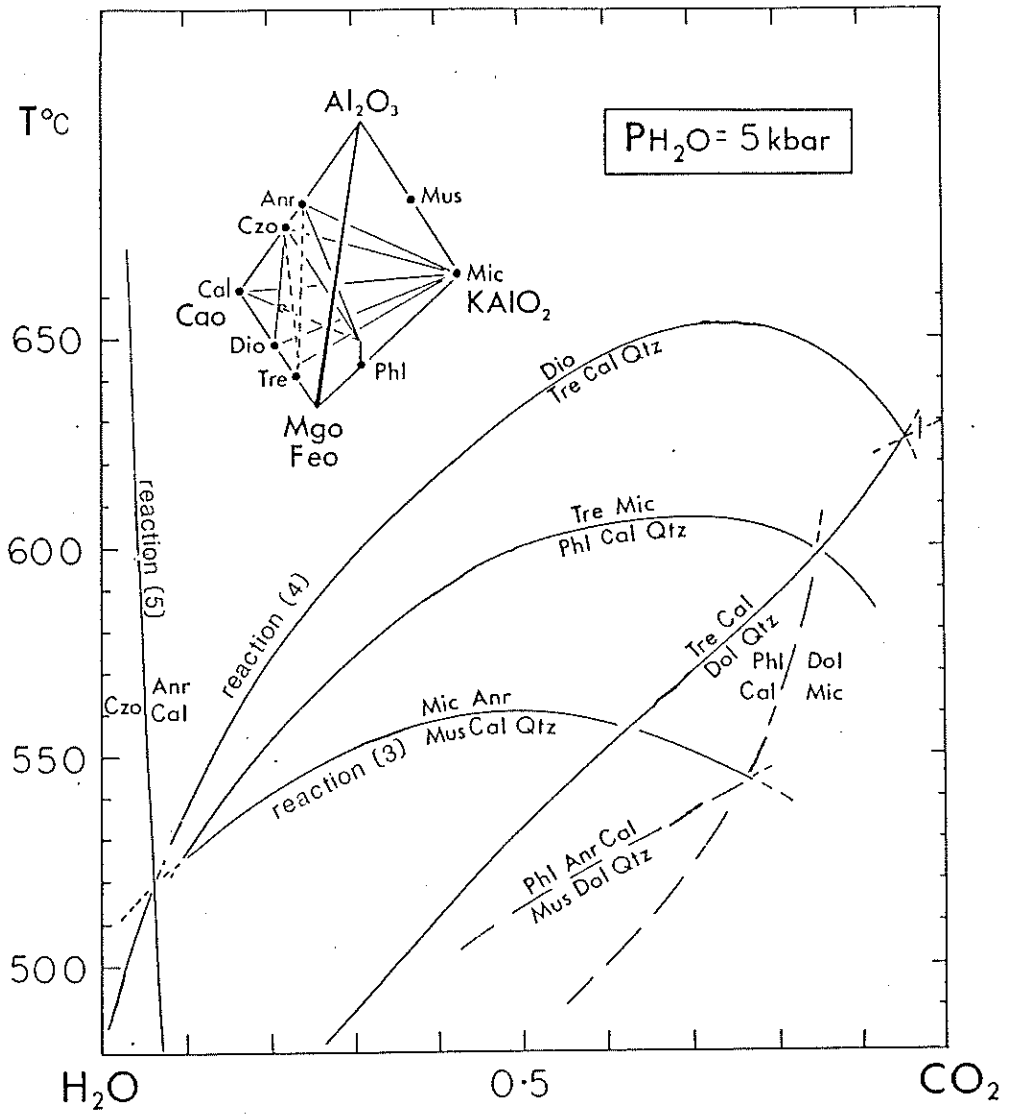
T°C
Al_2O_3
PH_2O= 5 kbar
Anr
Mus
Czo
Mic
$KAlO_2$
Cal
Cao
Dio
Tre
Phl
Mgo
Feo
650
600
550
500
reaction (5)
Czo
Anr
Cal
reaction (4)
Dio
Tre Cal Qtz
Tre Mic
Phl Cal Qtz
Tre Cal
Dol Qtz
Phl
Cal
Dol
Mic
Mic Anr
Mus Cal Qtz
reaction (3)
Phl Anr Cal
Mus Dol Qtz
H_2O
0·5
CO_2

fig.5

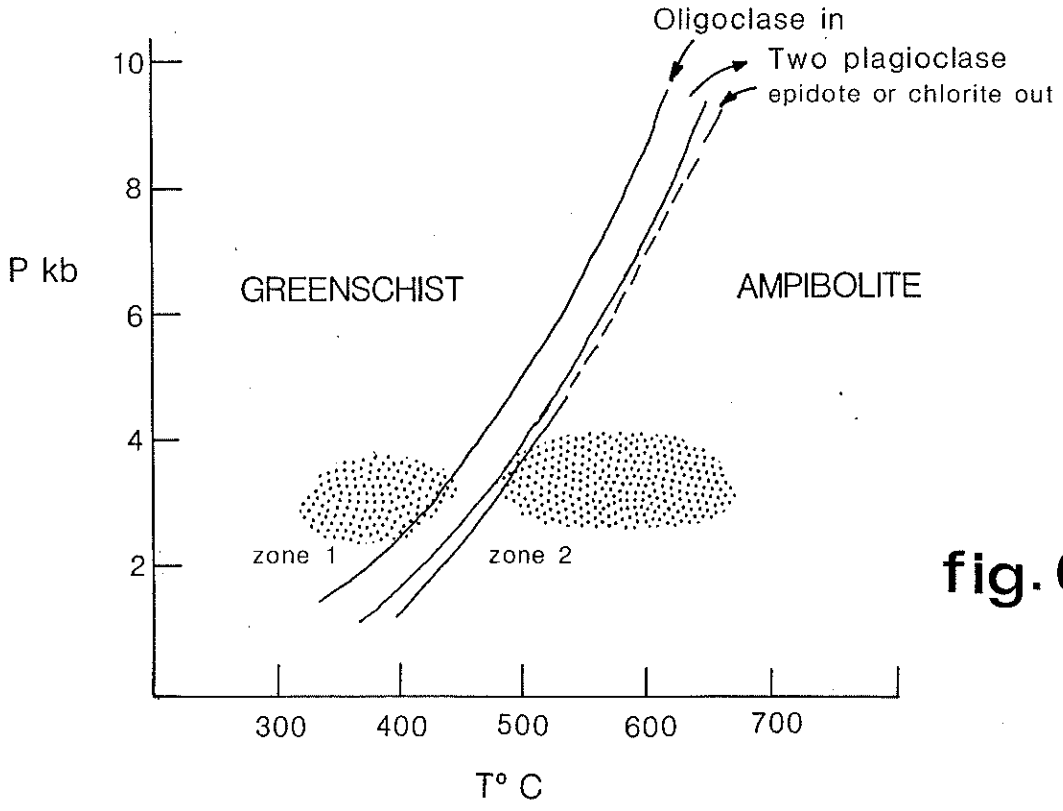
Oligoclase in
Two plagioclase
epidote or chlorite out
P kb
10
8
6
4
2
GREENSCHIST
AMPIBOLITE
zone 1
zone 2
300
400
500
600
700
T° C

fig.6

V. MINERAL CHEMISTRY

5.1 Introduction

A comparison of mineral chemistries in the study area is discussed using electron microprobe analysis data. Representative analyses may be found in Appendix 2.

5.2 Biotite Chemistry

Biotite is a common constituent in pelitic schists and metasiltstones. The composition of biotite is consistent in individual rocks, and although controlled by rock composition, biotite mineralogies can also be controlled by temperature (Binns, 1969).

Biotite within metasiltstones in zone 1 occurs as anhedral sheaves with weak pale tan (x) to pale brown (Y=Z) pleochroism and a high Mg/Mg+Fe ratio. Garnet-biotite assemblages show pale green to grass green pleochroism in subhedral elongate biotites from zone 1.

Amphibolites and garnet biotite schists from zone 2 show straw yellow to dark red brown pleochroism in biotites. The colour changes in biotite are related to the abundances of Ti and Fe (Binns, 1969). Green and pale brown biotites of zone 1 are the result of high Fe content relative to Ti, while red brown biotites in zone 2 have high Ti relative to Fe (Figure 7).

In garnet-biotite assemblages of similar bulk rock composition, trends in the Fe, Mg and Ti content of biotite may be the result of:

1) the preferential absorption of Fe into garnet, resulting in an increase in Mg/Fe ratio in coexisting biotite with an increase in garnet abundance with rising grade (Binns, 1965b).
2) the dominant acceptor for Ti in garnet-biotite assemblage is biotite, so that Ti must increase with grade as the total amount of biotite decreases.

5.3 Amphibole Chemistry

Amphiboles are common in both low and high grade rocks of basic and calcareous composition, ranging from tremolite to hornblende (Figure 8a).

Hornblende composition varies according to a number of factors (Leake, 1965a). Firstly, variation is mainly controlled by rock composition. Secondly, by the temperature of crystallization, and thirdly to metamorphic pressure. Comparison of amphiboles in metadolerites negates the first variable due to similarity of composition and makes comparison of the zones easier.

Figure 8b shows Na+K composition relative to Ti for hornblendes (after Zakrutkin, 1968). Two groups develop that are separated by the Greenschist-Amphibolite boundary. The variation of Ti is controlled by temperature (Binns, 1969, Raase, 1974), indicating that the two zones have been subjected to different temperature conditions. The calc-silicates show variable composition and is hampered by low Ti content in amphiboles of low grade.

Figure 8c (after Zakrutkin, 1968) of Al^{IV} vs. Al^{VI} for hornblende shows the development of two separate groups. The lower group lies within the Epidote Amphibolite Facies with lower Al^{IV}/Al^{VI} ratios which, according to Binns (1969) is pressure dependent. Grouping within the Epidote Amphibolite Facies instead of the Greenschist facies indicates moderate pressures. The groupings do not define accurately zones 1 and 2 but show intermixing. In several cases two different amphiboles are present in the same rock, with Na, K rich tremolite forming around hornblende during retrograde metamorphism. The lack of gradation between the two coexisting amphiboles is supportive evidence of the theoretical "jump" from tremolite to hornblende (Maruyama, 1983).

5.4 Garnet Chemistry

Garnets form during prograde metamorphism in pelitic schists and amphibolites. In zone 1 garnets in pelitic schists are associated with biotite, calcite and chlorite. They tend to be euhedral and inclusion free, with grainsize < 5mm. To the west in zone 2, garnet porphyroblasts up to 20mm are poikiloblastic and associated with hornblende, biotite, calcite, clinozoisite, microcline, plagioclase and quartz. Figure 9a shows garnet compositions are almandine ranging from ($Ca_{8.7-33.5}$ $Mn_{2.5-19.5}$ Fe_{53-84}) in zone 2 to ($Ca_{16.5}Mn_{25}Fe_{58}$) in zone 1.

Figure 9b shows CaO + MnO abundance relative to FeO + MgO. Garnet hornblende assemblages have high CaO + MnO and do not coincide with the grades of Sturt (1962). This feature may be controlled more by the rock chemistry than grade of metamorphism. Garnet amphibolites are rich in CaO and MnO in comparison to garnet biotite schists resulting in Ca, Mn rich garnet. The schists show a trend with increasing grade. Garnet-biotite schists of zone 1 with lower FeO + MgO plot in the biotite grade and show a trend towards higher FeO + MgO and a corresponding decrease in CaO + MnO in zone 2.

The decrease in Mn with increasing grade is due to the exclusion of the larger Mn ion (0.91Å radii) in preference for the smaller Fe^{2+} (0.83Å) and Mg^{2+} (0.87Å) (Sturt, 1962). Also garnet contains most of the Mn in the host rock (Binns, 1965b) and as garnet becomes more abundant with increasing grade, Mn in garnet must fall.

5.5 Plagioclase Feldspar Chemistry

Plagioclase compositions are widespread within the area, from An_0 to An_{46}. Plagioclase in metasediments and metadolerites within zone 1 are sodium rich (Ab_{100} - Ab_{97}) (Figure 8d). Garnet biotite schists within zone 2 show the highest calcium enrichment (An_{31} An_{46}) overlapping with plagioclase compositions from amphibolites (An_{16}-An_{32}), and the more variable calcsilicates (minor An_{35} with the majority An_0 - An_7). The orthoclase component in plagioclase is minor, commonly within 0-5%.

5.6 Summary

From the discussion of mineral compositions, several conclusions can be made:-

1) Bulk rock composition is the major factor in determining mineral composition
2) Within lithologies of similar composition changes in the minerals can be related to changes in metamorphic grade. The changes of particular interest are
   - (i) changes in biotite composition in garnet-biotite schists from high Mg/Mg+Fe ratio, low Ti in zone 1 to low Mg/Mg+Fe and high Ti within zone 2
   - (ii) low Ti, Na+K and AI^{VI} in amphiboles of basic rocks in zone 1 in contrast to high Ti, Na+K and AI^{VI} amphiboles in zone 2
   - (iii) garnet biotite schists show a trend from Ca, Mn rich garnets of zone 1 to Fe, Mg rich garnets of zone 2
   - (iv) plagioclase compositions show a jump from An_0 - An_3 in metadolerites of zone 1 to An_{16}-An_{32} in zone 2
   - (v) calc-silicates show wide variation in mineral compositions not always characteristic of the metamorphic facies involved and is likely to be due to variations in rock chemistry.

Figure 7

Mg/Mg + Fe ratio plotted against Ti content per formula unit for biotites within the study area

Figure 9a

Grossularite-almandine-spessartine compositions of garnets within the study area

Figure 9b

(CaO + MnO) vs. (FeO + MgO) weight percentages for garnets (after Sturt, 1962)

Fig.7

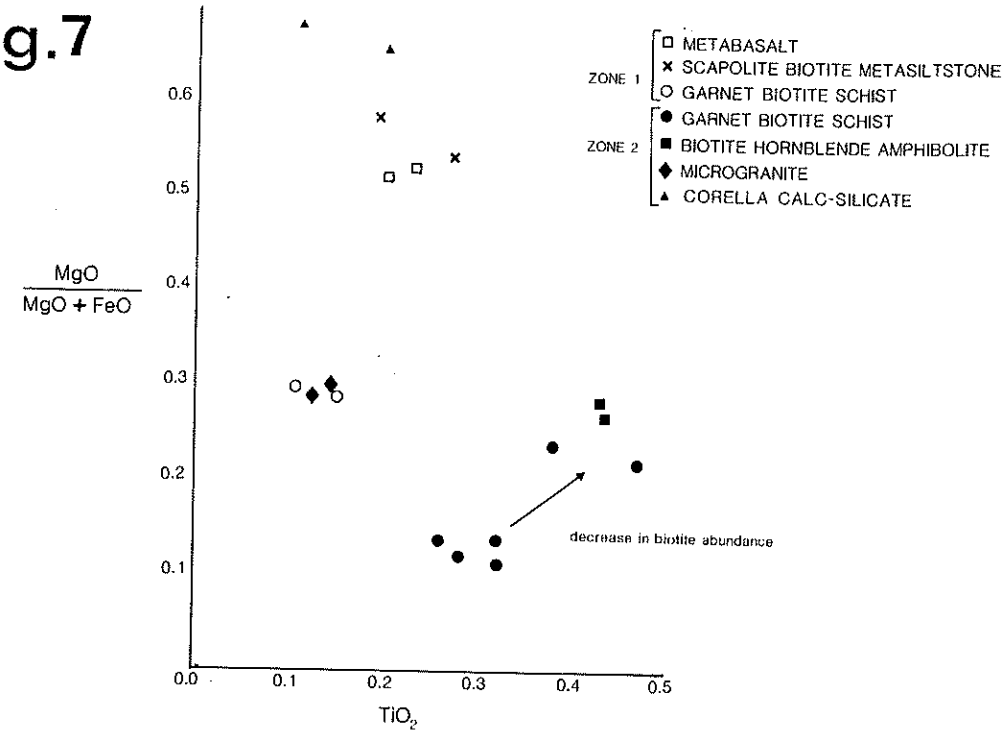
ZONE 1
METABASALT
SCAPOLITE BIOTITE METASILTSTONE
GARNET BIOTITE SCHIST
ZONE 2
GARNET BIOTITE SCHIST
BIOTITE HORNBLENDE AMPHIBOLITE
MICROGRANITE
CORELLA CALC-SILICATE
MgO / MgO + FeO
0.6
0.5
0.4
0.3
0.2
0.1
0.0
0.1
0.2
0.3
0.4
0.5
TiO2
decrease in biotite abundance

Fig.9

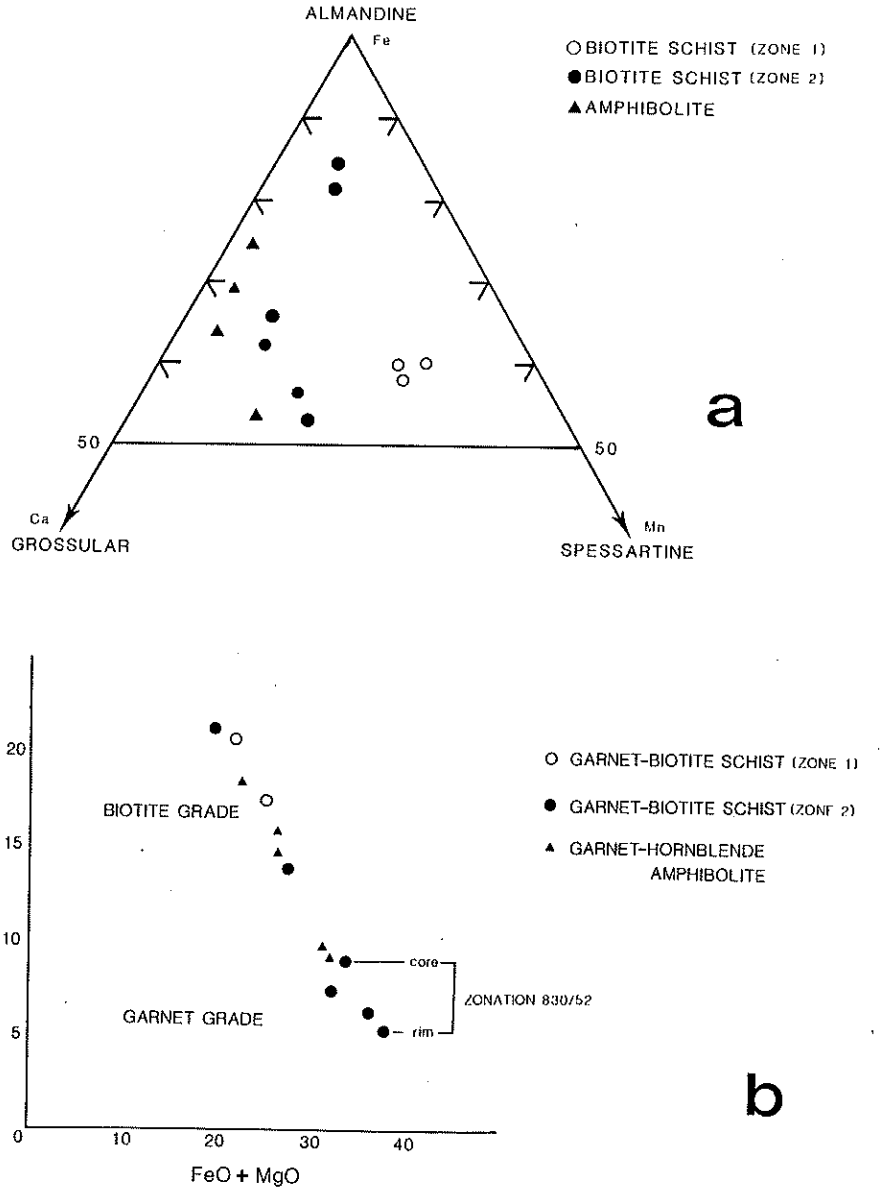
ALMANDINE
Fe
BIOTITE SCHIST (ZONE 1)
BIOTITE SCHIST (ZONE 2)
AMPHIBOLITE
50
50
Ca
GROSSULAR
Mn
SPESSARTINE
a
CaO + MnO
20
15
10
5
0
10
20
30
40
FeO + MgO
BIOTITE GRADE
GARNET GRADE
core
rim
ZONATION 830/52
GARNET-BIOTITE SCHIST (ZONE 1)
GARNET-BIOTITE SCHIST (ZONE 2)
GARNET-HORNBLENDE AMPHIBOLITE
b

Figure 8a

Compositional variation of calcic amphibole with regard to tetrahedrally coordinated aluminium and total alkalis per formula unit (after Deer et al. 1963)

Figure 8b

Plot of total alkali content vs. Ti content per unit formula (after Zakrutkin, 1968)

Figure 8c

Compositional variation of calcic amphiboles with regard to tetrehedrally and octahedrally coordinated aluminium (after Zakrutkin, 1968).

Figure 8d

Plagioclase compositions within rock types in the study area

fig.8

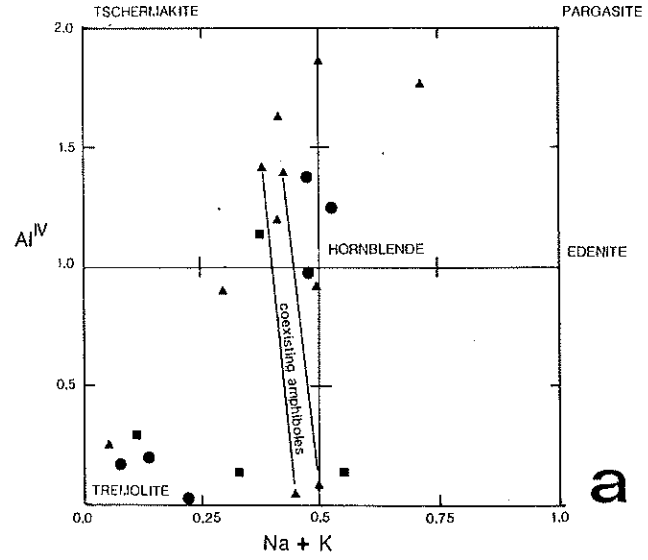
TSCHERMAKITE
PARGASITE
HORNBLENDE
EDENITE
coexisting amphiboles
TREMOLITE
Al^{IV}
Na + K
2.0
1.5
1.0
0.5
0.0
0.25
0.5
0.75
1.0

a

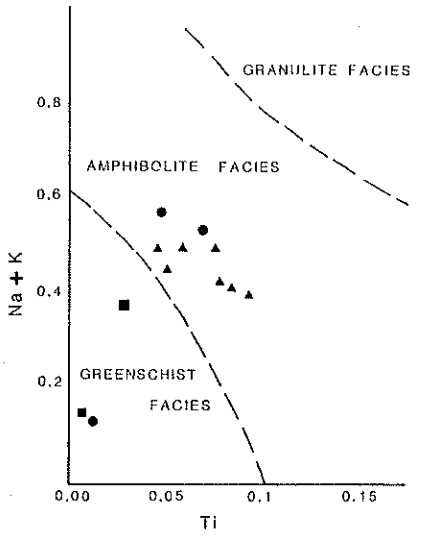
GRANULITE FACIES
AMPHIBOLITE FACIES
GREENSCHIST FACIES
Na + K
Ti
0.8
0.6
0.4
0.2
0.00
0.05
0.1
0.15

b

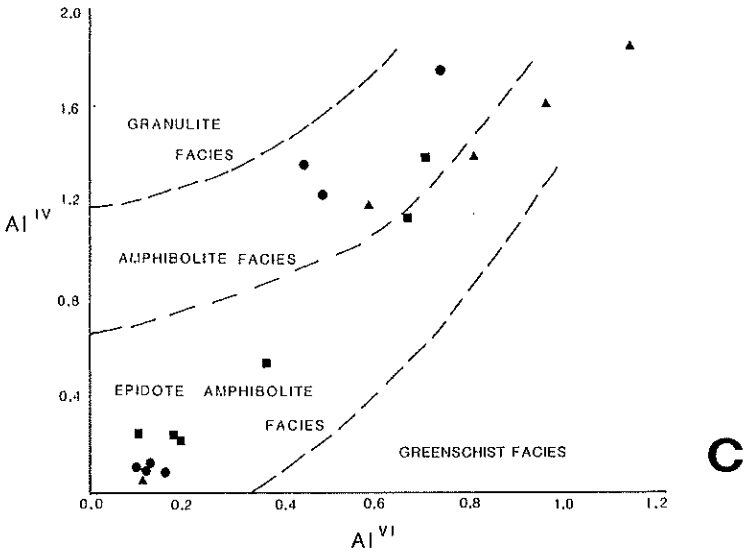
GRANULITE FACIES
AMPHIBOLITE FACIES
EPIDOTE AMPHIBOLITE FACIES
GREENSCHIST FACIES
Al^{IV}
Al^{VI}
2.0
1.6
1.2
0.8
0.4
0.0
0.2
0.4
0.6
0.8
1.0
1.2

c

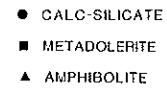
CALC-SILICATE
METADOLERITE
AMPHIBOLITE

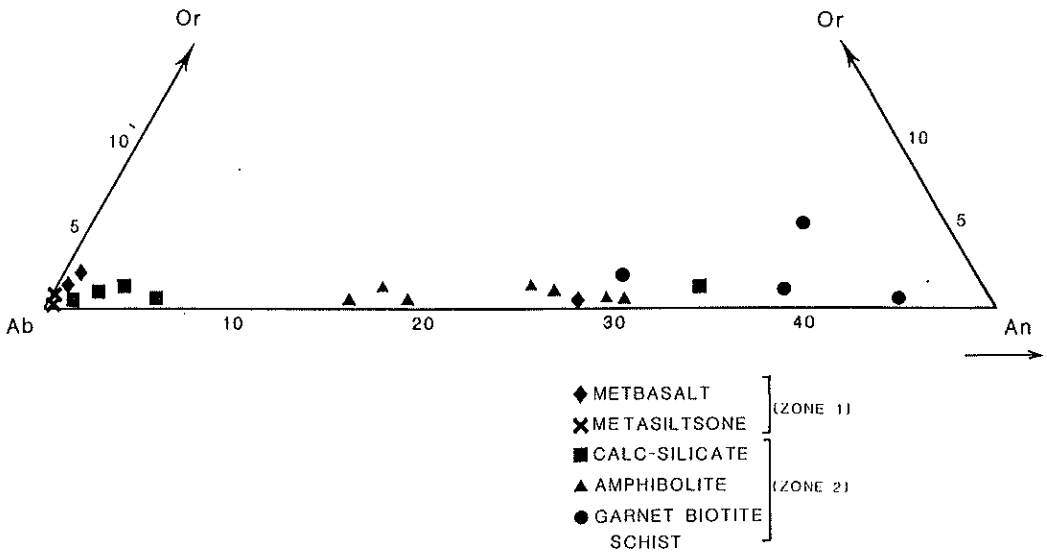
Or
Or
10
5
10
5
Ab
10
20
30
40
An
METBASALT
METASILTSONE
(ZONE 1)
CALC-SILICATE
AMPHIBOLITE
GARNET BIOTITE SCHIST
(ZONE 2)

d

VI. MAJOR ELEMENT GEOCHEMISTRY

6.1 Introduction

Presented here is a geochemical comparison of the Overhang Jaspilite, Corella Formation, Metadolerites and Amphibolites. Major element abundances of samples collected within the study area are given in Appendix II. Thin section descriptions and sample localities are given in Appendix I and Niggli, ACF values are presented in Appendix IV.

6.2 Major Element Geomchemistry of the Overhang Jaspilite Formation

The formation contains a wide variety of rock types, which is reflected by the geochemistry. In particular SiO_2 (7.5-97%), Al_2O_3 (0.08-20%), Fe_2O_3 (2-23%), MgO (0.04-18%), CaO (0.13-81%) and K_2O (0.01-7.5%). The plot of K_2O against Al_2O_3 (Figure 10b) shows a linear trend of K_2O enrichment for increasing Al_2O_3, reflecting the variation of low K_2O, Al_2O_3 in limestones and quartzites to high K_2O, Al_2O_3 in feldspathic and pelitic rock types.

Figure 10a shows a linear trend of enrichment of TiO_2 with increasing Al_2O_3, reflecting the abundance of biotite in various rock types. MgO content lies within narrow limits compared to large variations in K_2O (Figure 10e) while the ternary Al_2O_3 - Fe_2O_3 - K_2O (Figure 10i) shows a strong trend reflecting the pelitic composition of the rocks.

The geochemical trends of the suite suggests the source region is fairly constant, particularly detritus input due to the interdependence of Fe, Al and K, the common constituents of clays and micas.

6.3 Major Element Geochemistry of the Corella Formation

As with the Overhang Jaspilite, a wide variation in rock types is also characteristic of the Corella Formation. The calc-silicates show major element variation from 33-53% SiO_2, 7-16% Al_2O_3, 5-24% Fe_2O_3, 4.5-7% MgO, 8-23% CaO and 0.5-7% K_2O. Schists and Quartzites show higher SiO_2 (63-82%), similar Al_2O_3 (9.5-18%), Fe_2O_3 (1.71-14%), K_2O (0.7-10%) and lower MgO (0.0-8.6%) and CaO (0.1-4%) compared to the calc-silicates.

Figures 10a,b show the samples plot near the sedimentary trend of the Overhang Jaspilite although variations include high values of TiO_2 for two samples, and low K_2O values of the pelitic schists and calc-silicates. Figures 10e,f,g show the distinction of pelitic schists and quartzites from calc-silicates by lower MgO, CaO and higher SiO_2. The more linear trend defined by the Na_2O, MgO, K_2O ternary diagram (Figure 10h) shows that these elements are inter-related and suggests an evaporitic environment of deposition with high salt and dolomite content.

6.4 Major Element Geochemistry of the Amphibolites and Metadolerites

Within the metadolerites, variations in major elements are small, SiO_2 (48.5 -56%), Al_2O_3 (12-17%), Fe_2O_3 (12-17.5%), MgO (2-8%), CaO (2-10%), Na_2O (2.4-4%), K_2O (0.2-2.5%) and TiO_2 (0.9-2.3%). Some amphibolites have lower MgO, higher MnO and Fe_2O_3 than metadolerites. The variations can be explained by differentiation trends shown on the Niggli 100 mg -c - (al-alk) diagram (Figure 11b). Two samples show higher TiO_2, MnO and lower MgO, Na_2O content. The high TiO_2 of the samples suggests the changes are not due to metamorphism but are related to later stages of differentiation.

The ACF plot (Figure 11c) shows that the metadolerites plot within a narrow field and are similar geochemically to the Corella calc-silicates. Figure 10c shows the Ti content of dolerites deviates greatly from the sedimentary trend of Figure 10a.

6.5 Comparitive Geochemistry

The comparison of the Overhang Jaspilite and the Corella Formation, which broadly coincide with zones 1 and 2 respectively, may be useful in showing changes in bulk rock chemistry during metamorphism. To do this, it is necessary to determine if the two formations are of geochemically similar origins. Plotted on the Niggli 100 mg-c-(al-alK) diagram (Figure 11a), the two formations show similarities in original rock types.

The plot of TiO_2 against Al_2O_3 (Figure 10a) shows that the two formations plot along the same trend. TiO_2 is expected to be fairly immobile and unchanged during metamorphism. Therefore the two formations appear to be derived from detrital sources of similar Al_2O_3 and TiO_2. High TiO_2 values in some Corella samples indicate an igneous origin (Walker, 1960) and may be strongly altered dolerites that have developed characteristics of calc-silicates by the introduction of mobile elements through metasomatism. Distinction using preserved relict igneous textures is not possible in these samples as all original textures are destroyed by metamorphism.

The plot of K_2O vs. Al_2O_3 shows that calc-silicates and pelitic schists plot close to the trend defined by the Overhang Jaspilite but show lower K_2O content. This feature can be related to the loss of K_2O during metamorphism, due to the high mobility of K_2O with increasing temperatures (Orville, 1969). Other distinctions between the two formations are the wide variation in CaO, Na_2O and MgO values of the Corella Formation. Calc-silicates show higher Ca and Mg than pelitic schists and quartzites, which is reflected in the different mineral assemblages of the two rock types. The lack of graduation between the two types is contrary to the trend observed in the Overhang Jaspilite and suggests a loss of Mg, Ca from the pelitic schists and a nett gain in the calc-silicates.

The high mobility of Ca, Mg, Na during metamorphism (Orville, 1969) indicates the inter-relationships of Na_2O, MgO and K_2O (Figure 10h) in the calc-silicates may be due to metasomatic processes. The environment of deposition of the Corella Formation has been suggested by Derrick (1971) to be evaporitic, therefore the abundance of Na and Mg may be related to halite and dolomite formation rather than metasomatism. The presence of Cl rich scapolite in calc-areous rocks supports this idea (Ramsay et al. 1970).

The Corella schists, with lower MgO content than the calc-silicates are not derived from evaporitic environments and are not expected to show the influence of the depositional environment. They are therefore expected to show similarities to pelitic rocks of the Overhang Jaspilite where Mg content is likely to be influenced mainly by the source region. The fact that Corella schists show lower MgO than the Overhang Jaspilite may suggest the loss of Mg by metamorphic processes. This would require movement of Mg against a chemical gradient into Mg-rich calc-silicates and amphibolites. Dehydration reactions within the schists could provide enough fluid pressure to allow for mass transport of mobile elements out of the schists, particularly strongly foliated schists. High permeability due to a volume decrease during devolitization and the development of microcracks in grains due to high stress allows for large amounts of fluid to pass through the rock (Etheridge, 1983). The samples of schists obtained are closely associated with the Tommy Creek Microgranite. Outgassing of H_2O from the granite during crystallization is also a possible source of fluid (Ferry, 1978) and would provide a pressure gradient to drive fluids out of the schists.

Calc-silicates and dolerites are geochemically similar, and plot in a narrow field on the ACF diagram (Figure 11c), resulting in the development of similar mineralogies in the two rock types at high grades of metamorphism. The distinction of amphibolites of sedimentary and igneous origin within north west Queensland has been the subject of studies by Walker (1960). Various methods of distinction did not result in conclusive distinctions between amphibolites. Within the study area geochemical distinction of amphibolites is easily obtained in most cases by the high Ti content of amphibolites of igneous origin.

Figure 10a

TiO_2 WT % vs. Al_2O_3 WT % for Corella calc-silicates and schists and various lithologies of the Overhang Jaspilite

Figure 10b

K_2O WT % vs Al_2O_3 WT % for Corella calc-silicates and schists and various lithologies of the Overhang Jaspilite

Figure 10c

TiO_2 WT % vs. Al_2O_3 WT % for metadolerites and amphibolites

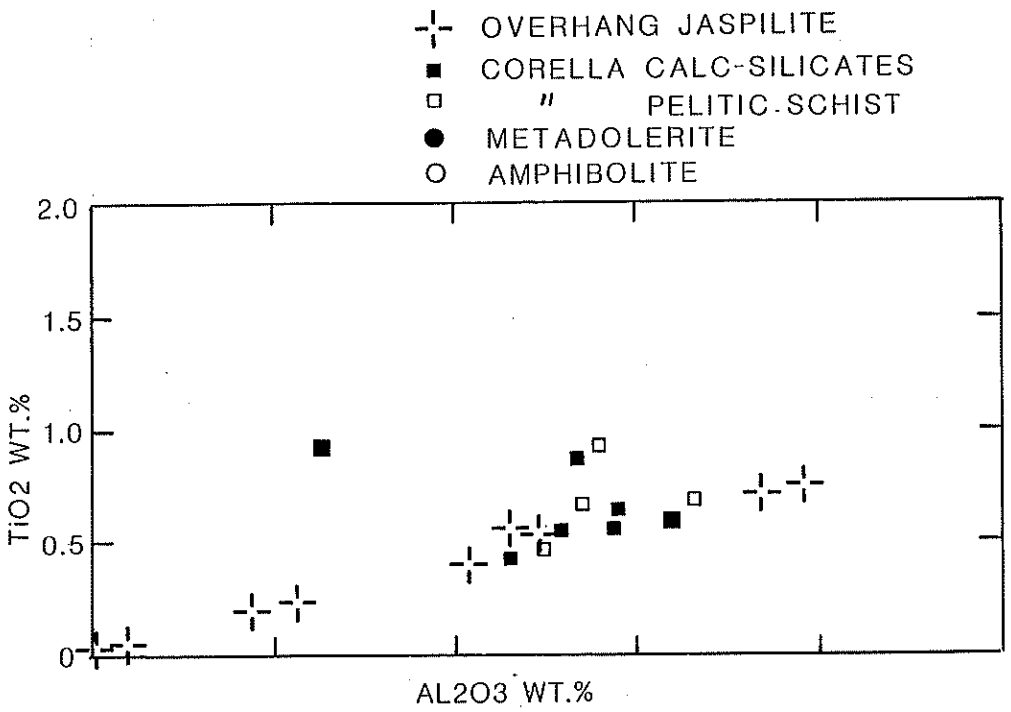

fig.10a

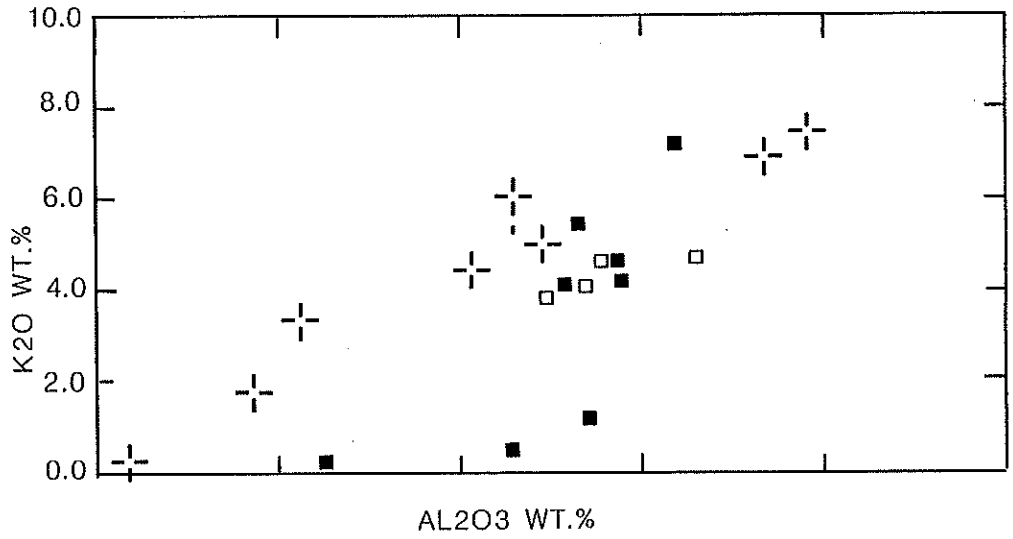

fig.10b

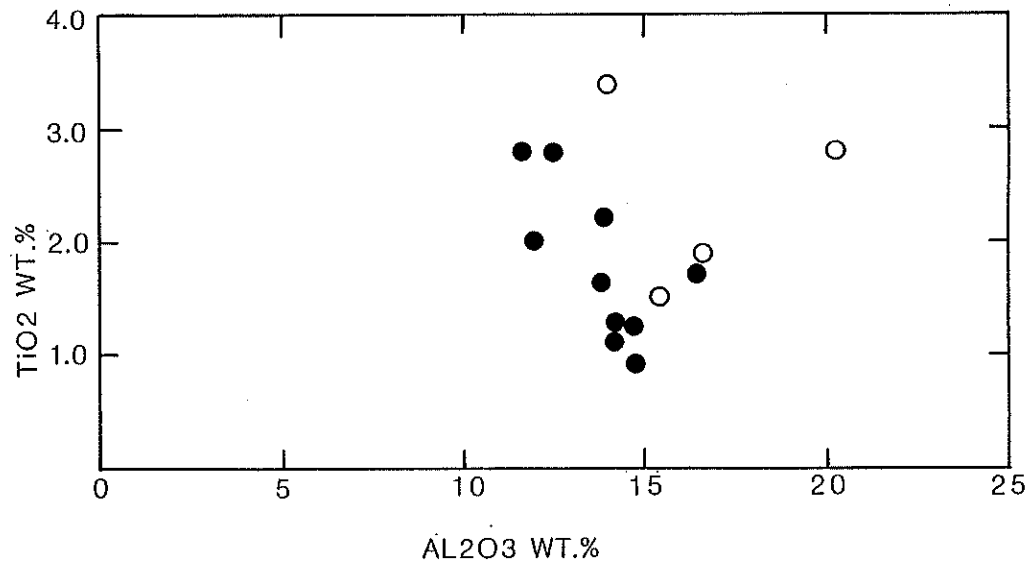

fig.10c

Figure 10d

MgO WT % vs. SiO_2 WT % for Corella calc-silicates and pelitic schists and Overhang Jaspilite

Figure 10e

K_2O WT % vs. MgO WT % for Corella calc-silicates and pelitic schists and Overhang Jaspilite

Figure 10f

Al_2O_3 WT % vs. SiO_2 WT% for Corella calc-silicates and pelitic schists and Overhang Jaspilite

Figure 10g

Na_2O WT % vs. CaO WT% for Corella calc-silicates and pelitic schists and Overhang Jaspilite

Figure 10h

Na_2O - MgO - K_2O WT % ternary diagram for Corella calc-silicates and pelitic schists and Overhang Jaspilite

Figure 10i

K_2O - Al_2O_3 - Fe_2O_3 WT% ternary diagram for Corella calc-silicates and pelitic schists and Overhang Jaspilite.

fig.10 contd.

× OVERHANG JASPILITE
■ CORELLA CALC-SILICATE
□ " PELITIC SCHIST
● " QUARTZITE

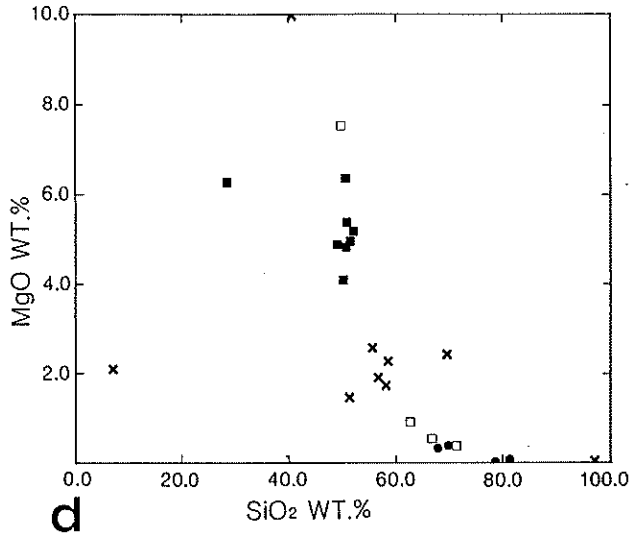

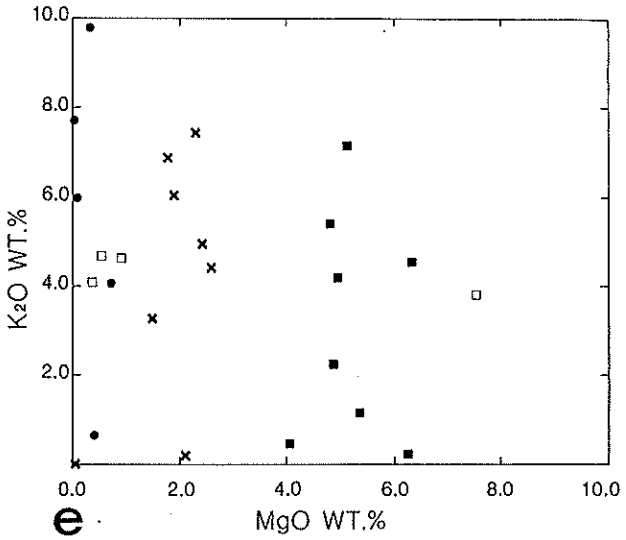

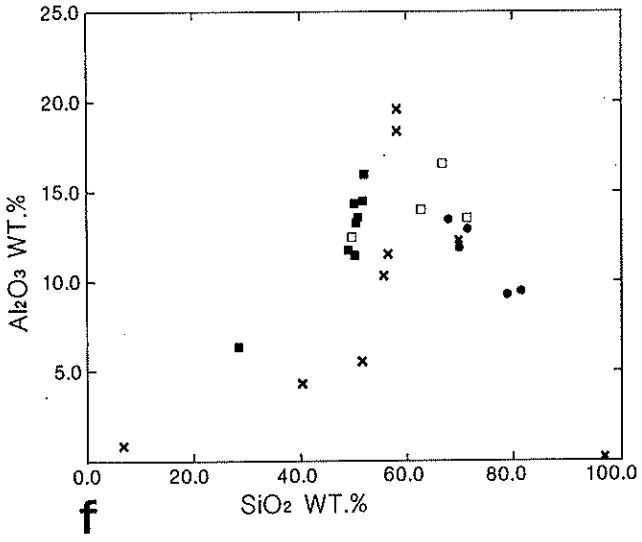

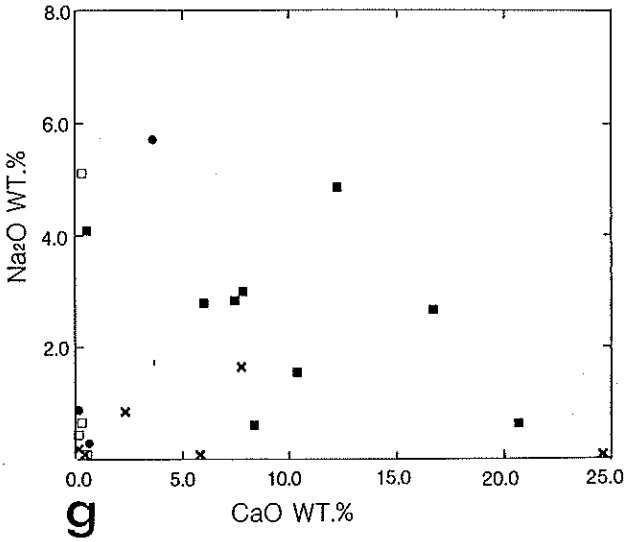

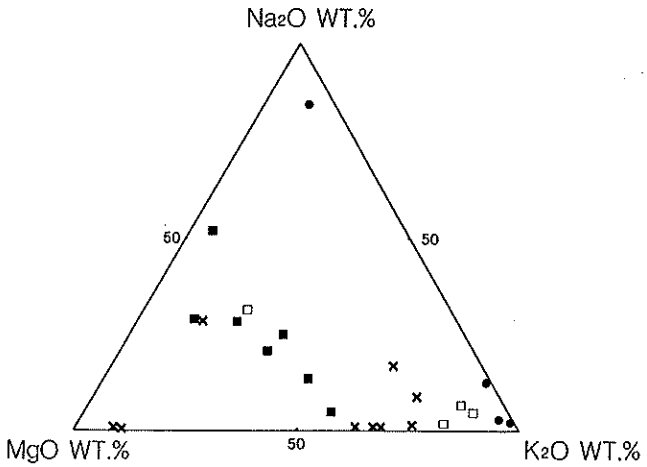

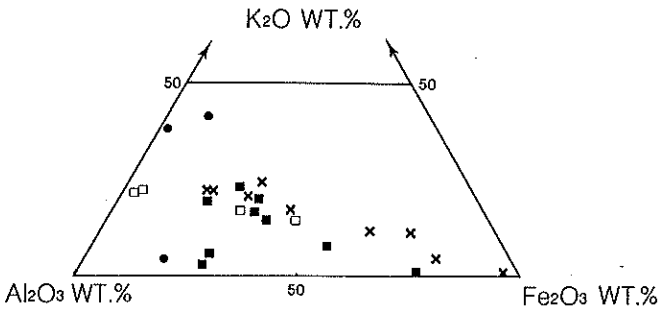

Figure 11a

Niggli c - 100mg - (al - alK) ternary diagram for metasediments in the study area (after Leake, 1964)

Figure 11b

Niggli c - 100 mg - (al-alK) ternary diagram for metadolerites, amphibolites and microgranite in the study area (after Leake, 1964)

Figure 11c

ACF diagram for metasediments and dolerites within the study area

fig. 11

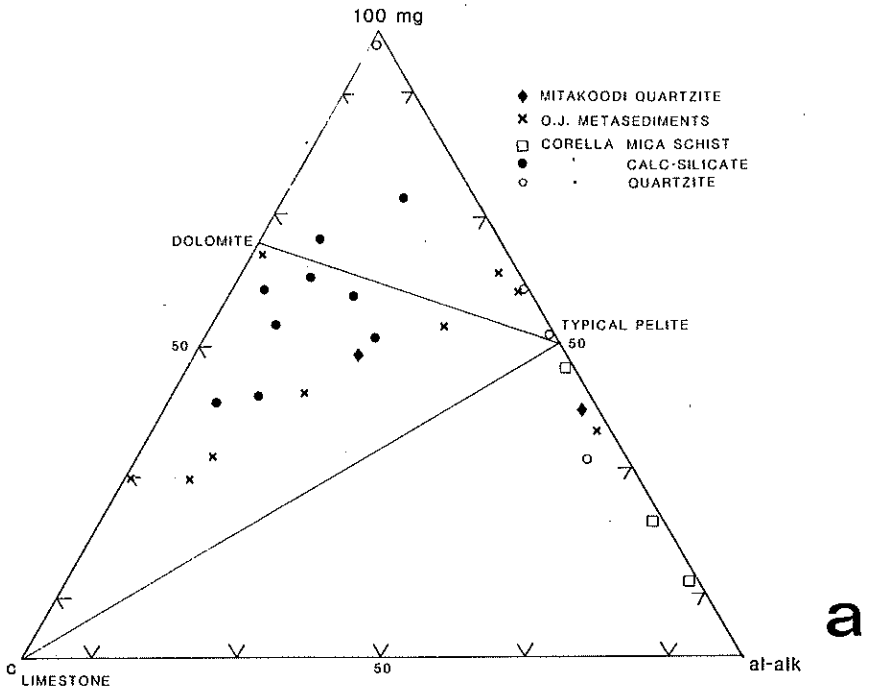
100 mg
MITAKOODI QUARTZITE
O.J. METASEDIMENTS
CORELLA MICA SCHIST
CALC-SILICATE
QUARTZITE
DOLOMITE
TYPICAL PELITE
50
50
C
LIMESTONE
50
al-alk

a

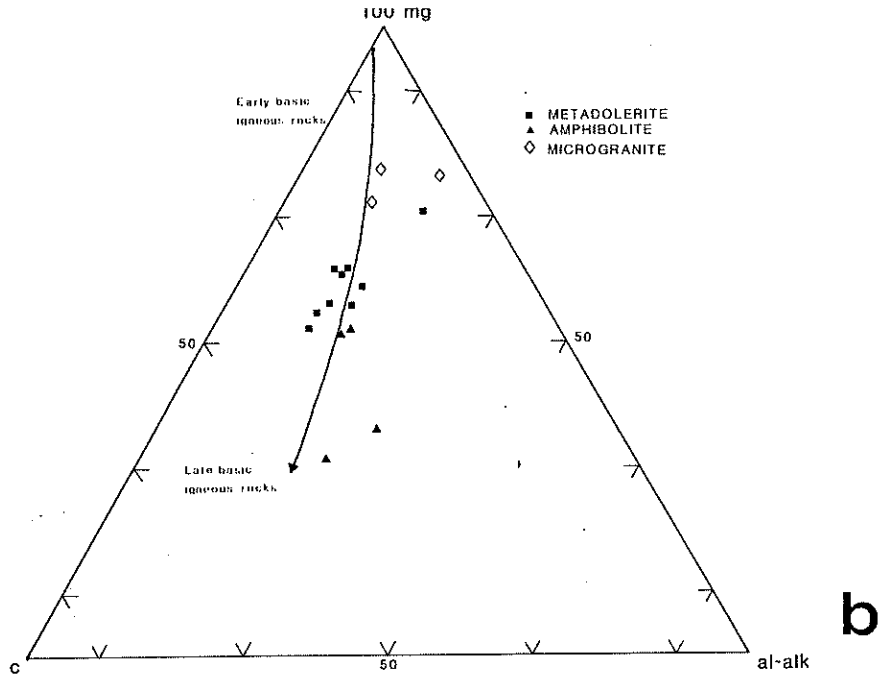
100 mg
Early basic igneous rocks
METADOLERITE
AMPHIBOLITE
MICROGRANITE
50
50
Late basic igneous rocks
C
50
al-alk

b

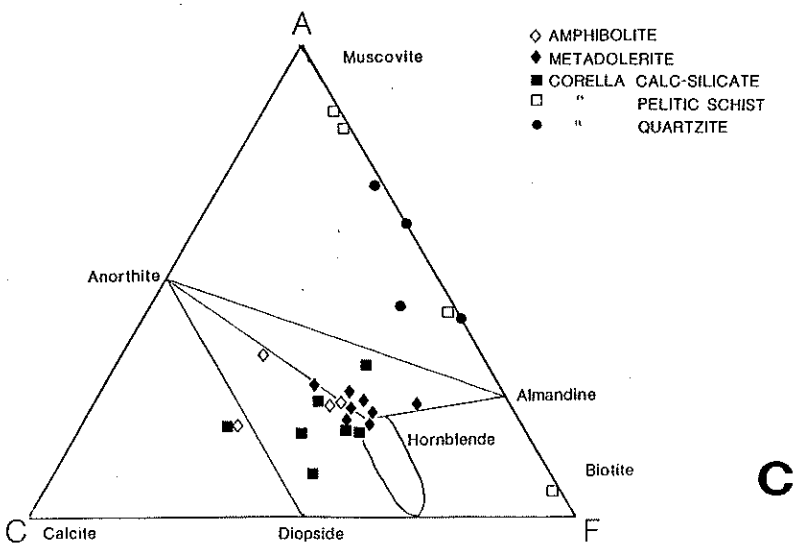
A
Muscovite
AMPHIBOLITE
METADOLERITE
CORELLA CALC-SILICATE
" PELITIC SCHIST
" QUARTZITE
Anorthite
Almandine
Hornblende
Biotite
C
Calcite
Diopside
F

c

VII. DISCUSSION

Bulk rock - Mineral compositions

The geochemical differences between the Corella Formation and the Overhang Jaspilite, discussed in Chapter VI, may be related to the environment of deposition, due to the high Mg, Ca and Na content of the calc-silicates of the Corella Formation, in comparison to the calcareous granofels of the Overhang Jaspilite. Detrital input for the two units appears to be from a fairly constant source.

The differences in rock chemistry should be reflected in mineral compositions, but are also affected by the differences in metamorphic grade.

The high Mg content in the calc-silicates within zone 2 is reflected in Mg rich biotites, similarly, the lower Mg content in pelitic schists is reflected in Mg deficient biotites. Trends within garnet-biotite assemblages of similar bulk rock composition show a decrease in Mg and an increase in Ti in biotites from zone 1 to zone 2, which is related to temperature and not changes in bulk rock composition.

Garnet shows a trend of decreasing CaO + MnO content with increasing FeO + MgO content from zone 1 to zone 2 which is particularly noticable in garnet-biotite schists. The changes are related to increasing temperature, as opposed to garnets within zone 2, with high CaO + MnO reflecting the abundance of Ca and Mn in the original rock.

Amphiboles of tremolite and hornblende compositions are common in metamorphosed calcareous rocks and metadolerites in zone 2, while only tremolite is found in these rock types in zone 1. The similarity in bulk rock compositions of metadolerites across the study area, and the large variation in amphibole compositions shows that metamorphic conditions are more important in determining amphibole composition than bulk rock composition. Hornblendes in zone 2 are richer in Al, Na, K and Ti than tremolites. Prograde tremolite can be distinguished from retrograde tremolite in zone 2 by higher Na + K content, probably the result of a preferential loss of Al from hornblende and the retention of Na and K within the structure.

Plagioclase shows a marked variation in composition across the study area. Albite characterises plagioclase in zone 1 in basic and pelitic rocks. In zone 2 Anorthite content increases with temperature and values range up to An_{46}. Bulk rock composition does not play an important role in plagioclase compositions. Garnet biotite schists with low Ca content have Ca rich (An_{31} - An_{46}) plagioclases. Albite is the common plagioclase in calc-silicates although this feature is the result of retrograde reactions converting Ca plagioclase to zoisite and albite.

Mineral Paragenesis

One of the aims of this thesis was to determine a sequence of metamorphic and structural events, which are discussed in Chapter IV. Mineral development can be associated with particular events to provide a complete picture of the metamorphic history of the area (see Figure 12).

Within zone 1 mineral assemblages indicate metamorphism typical of the Upper Greenschist Facies, which is reflected in geothermometer temperatures of 430-480°C. Pre D_1 mineral development includes scapolite, biotite, tremolite in calcareous rocks and metasiltstones and biotite with minor garnet in pelites. Biotite development continued during the development of the S_1 foliation at high angles to the bedding. No M_2 mineral growth has been detected in zone 1, indicating metamorphism is localised. Retrograde metamorphism resulted in only minor alteration of minerals and is evidenced mainly by the development of chlorite and epidote.

Within zone 2 the growth of minerals associated with contact metamorphism around the Tommy Creek Microgranite has been obscured by regional metamorphism of Almandine Amphibolite Facies, with the genesis of hornblende, garnet, calcium plagioclase and biotite in basic rocks, diopside and tremolite in calcareous rocks, and biotite, garnet and muscovite in pelitic rocks.

The pre- and syntectonic development of garnets and the development of a strong foliation in pelitic and basic rocks, suggests continued growth of most prograde minerals possibly accompanied by mechanical rotation of early formed minerals during isoclinal folding. Only minor zoning is present in garnets related to M_1, suggesting re-equilibration of the cores and rims during metamorphism.

The development of north-east trending F_2 folds in zone 2 is associated in time to the intrusion of the Naraku Granite. Mineral growth is limited to contact aureoles and isolated "hot spots", probably overlying granite intrusions. Garnet growth during this event indicates temperatures reached those of the regional metamorphism. However, due to the limited penetration of this metamorphic event a great variation in temperature is evident. Contact aureoles in calc-silicates show an abundance of diopside, and the development of potassium feldspar porphyroblasts in pelitic schists are also related to this event.

Retrograde metamorphism in this zone is indicated by the growth of zoisite and epidote in calcareous rocks, sericitization of plagioclase, the development of chlorite in garnets, and tremolite rims around hornblendes in amphibolites. The calculated pressures of H_2O and CO_2 during metamorphism indicate that X_{H2O} dominated during retrograde metamorphism. The suggested high X_{CO2} in calc-silicates during

prograde metamorphism would have been reduced considerably to allow zoisite to form from anorthite (reaction (5) p.18), the lack of calcium plagioclase in most calc-silicates suggests widespread zoisite formation. The calculated temperature of retrograde metamorphism (~ 420°C) is suitable for the formation of chlorite, tremolite and epidote as well, presumably under high X_{H2O} conditions. The influx of water would have been aided by devolitization and decarbonation reactions (Thompson (1975)), causing a reduction in rock volume and hence increased permeability.

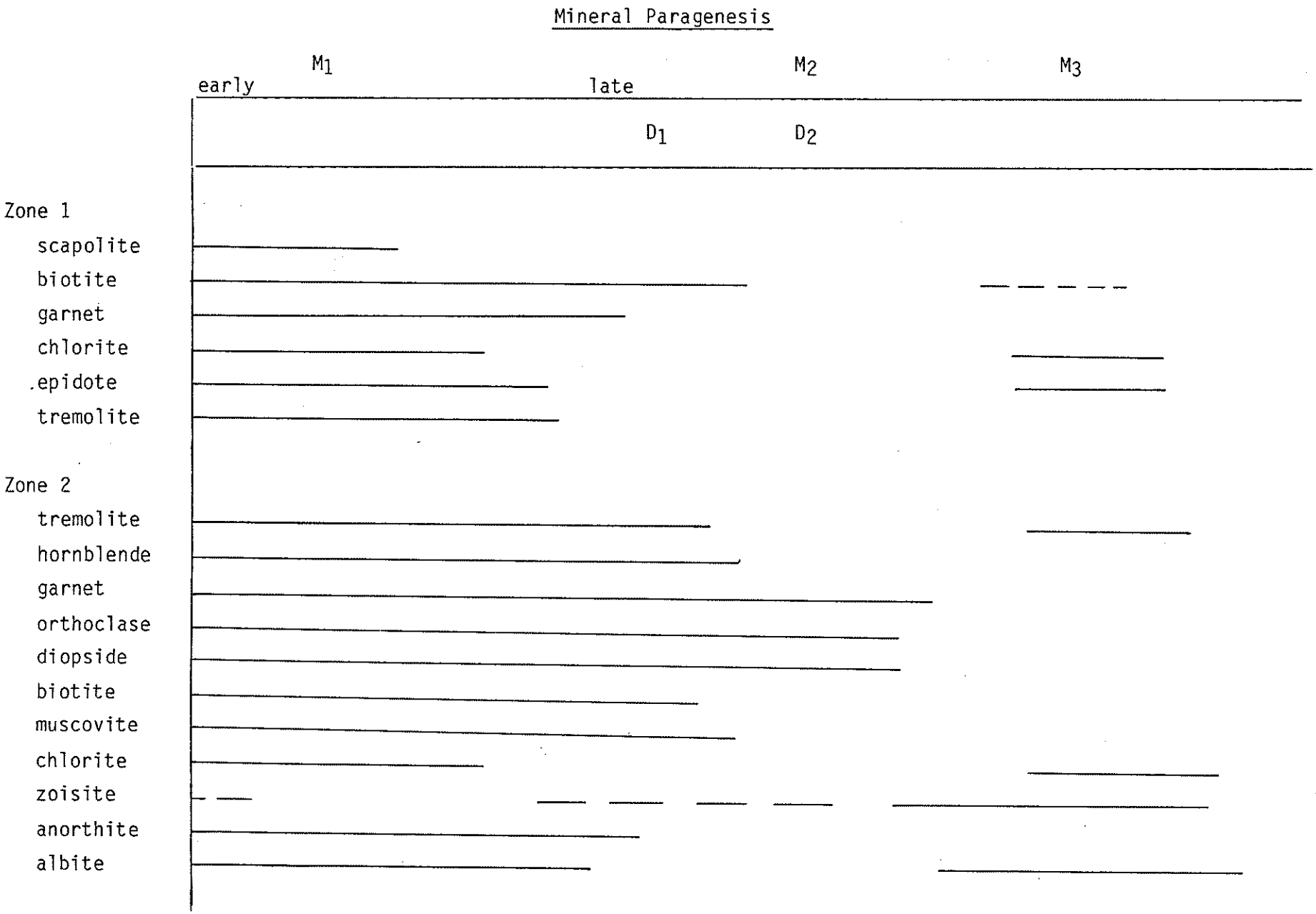
Mineral Paragenesis
M1
M2
M3
early
late
D1
D2
Zone 1
scapolite
biotite
garnet
chlorite
epidote
tremolite
Zone 2
tremolite
hornblende
garnet
orthoclase
diopside
biotite
muscovite
chlorite
zoisite
anorthite
albite

Fig.12

ACKNOWLEDGEMENTS

The writer is indebted to Prof. Peter Ypma for the initiation of this project and for providing encouragement and invaluable assistance throughout the year.

The writer would also like to thank Drs. Mike Etheridge and Gordon Lister for their helpful supervision in the field and later by correspondence from the Bureau of Mineral Resources, Canberra.

Drs. John Foden and Robin Oliver must also be thanked for providing greatly appreciated advice and comments during the year.

Acknowledgements go to Dr. B. Griffin for his assistance with electron microprobe analyses, J. Stanley and P. McDuie for assistance with geochemical data and G. Trevelyn and W. Mussared for the speedy production of thin sections.

Especial thanks goes to Judi Hurley for the professional and speedy typing of this thesis.

Final thanks are to my parents for their understanding and support throughout my education.

REFERENCES

Blake, D.H. (1980). The early geological history of the Proterozoic Mount Isa Inlier, northwestern Queensland : an alternative interpretation.

Binns, R.A. (1969). Ferromagnesian minerals in high-grade metamorphic rocks. Spec.Publ.Geol.Soc.Aust. 2, pp. 323-332.

Carter, E.K., Brooks, J.H., and Walker, K.R. (1961). The Precambrian mineral belt of northwestern Queensland. Bur.Miner.Resour.Aust.Bull. 51.

Deer, W.A., Howie, R.A., and Zussman, J. (1966). An Introduction to the Rock Forming Minerals. Longman Group Ltd., England.

Derrick, G.M., Wilson, I.H., Hill, R.M., and Mitchell, J.E., (1971) Geology of the Marraba 1:100 000 Sheet Area Queensland. Bur.Miner.Resour.Aust. Rec. 1971/56.

Derrick, G.M., and Wilson, I.H. (1975) Evolution of Proterozoic topography and the formation of mineralized basins in northwest Queensland; in Proterozoic Geology, abstracts of 1st Australian Geological Convention, Adelaide, 12-16 May, 1975, Sydney, Geol. Soc. Aust.

Derrick, G.M., Wilson, I.H. and Hill, R.M. (1976c) Revision of stratigraphic nomenclature in the Precambrian of northwest Queensland. III : Mount Isa Group. Qld.Govt.Min.J., 77, pp.402-5.

Etheridge, M.A., Wall, V.J., Vernon, R.H. (1983) The role of the fluid phase during regional metamorphism and deformation. J.Met.Geol. 1983. 1. pp. 205-226.

Fanning, C.M. (1980) Coexisting pyroxene geothermometry and garnet biotite geothermometry programs, University of Adelaide.

Ferry, J.M. (1976b) P, T, F_{CO2}, and f_{H2O} during metamorphism of calcareous sediments in the Waterville-Vassalboro area, south-central Maine. Contrib. Mineral.Petrol., 57, pp.119-143.

Ferry, J.M. (1978) Fluid interaction between granite and sediment during metamorphism, south-central Maine. Am.J.Sci. 278, pp.1025-1056.

Ferry, J.M. and Spear, F.S. (1978) Experimental calibration of the partitioning of Fe and Mg between biotite and garnet. Contrib.Mineral.Petrol. 66, pp. 113-117.

Glikson, A.Y., Derrick, G.M., Wilson, I.H. and Hill, R.M. (1976) Tectonic evoluation and crustal setting of the middle Proterozoic Leichardt River fault trough Mount Isa region, northwest Queensland. BMR Journ.Geol. Geophys., 1, pp.115-129.

Glikson, A.Y. (1980) Precambrian sial-sima relations : evidence for earth expansion. Tectonophysics, 63, pp.193-234.

Goldmann, D.S. and Albee, A.L. (1977) Correlation of Mg/Fe partitioning between garnet and biotite with $^{18}O/^{16}O$ partitioning between quartz and magnetite. Am.J.Sci., 277, pp.750-767.

Graham, C.M. and Powell, R. (1984). A garnet-hornblende geothermometer : calibration, testing and application to the Pelona Schist, Southern California. J.Met.Geol., 2, pp.13-31.

Klemm, M. (1975) Geology of the Lalor Prospect Area, University of Queensland. Hons. Thesis (unpublished)

Maruyama, S., Suzuki, K., Liou, J.G. (1983) Greenschist-Amphibolite Transition Equilibria at low pressures. J.Pet. 24; pp.583-604.

Orville, P.M. (1969) A model for metamorphic differentiation origin of thin layered amphibolites. Am.J.Sci., 267, pp.64-86.

Page, R.W. (1978) Response of U-Pb zircon and Rg-Sr total-rock and mineral systems to low-grade regional metamorphism in Proterozoic igneous rocks, Mount Isa, Australia. J.Geol.Soc.Aust., 25, pp.141-164.

Page, R.W. (1983b) Timing of superimposed volcanism in the Proterozoic Mount Isa Inlier, Australia. Prec.Res. 21, pp.223-245.

Plumb, K.A., Derrick, G.M. and Wilson, I.H. (1980) Precambrian geology of the McArthur River - Mt. Isa Region, northern Australia. In : Henderson, R.A., and Stephenson, P.J. (eds.), The geology and geophysics of northeastern Australia. Geol.Soc.Aust., Qld.Div., pp.71-88.

Raase, P. (1974) Al and Ti contents of Hornblende, Indicators of Pressure and Temperature of Regional Metamorphism Contr.Mineral Petrol., 45, pp.231-236.

Ramsay, J.G. (1967) Folding and Fracturing of Rocks. McGraw-Hill, New York, 568pp.

Robie, R.A., Hemmingway, B.S. and Fisher, J.R. (1978) Thermodynamic properties of minerals and related substances at 298.15°K and 1 bar (10^5 pascals) pressure and at higher temperatures. U.S.Geol.Surv.Bull., 1452.

Ryzhenko, B.N. and Malinin, S.D. (1971) The fugacity rule for the systems CO_2-H_2O, CO_2-CH_4, CO_2-N_2, and CO_2-H_2. Geochem.Int. 8, pp.899-913.

Saxena, S.K. (1969). Silicate solid solution and geothermometry : 3. Distribution of Fe and Mg between coexisting garnet and biotite. Contrib. Mineral. Petrol. 22, pp.259-267.

Spear, F.S. (1981). An experimental study of hornblende stability and compositional variability in amphibolite. Am.J.Sci., 281, pp.697-734.

Sturt, B.A. (1962) The composition of garnets from pelitic schists in relation to the grade of regional metamorphism. J.Petrol. 3, pp.181-191.

Thomas, A. (1984) Petrological and Fluid Inclusion Study of Lake Corella region Mt. Isa Inlier, northwest Queensland. Hons. Thesis, University of Adelaide.

Thompson, A.B. (1975). Calc-silicate diffusion zones between marble and pelitic schist. J.Petrol., 16, pp.314-346.

Thompson, A.B. (1976). Mineral reactions in pelitic rocks : II Calculation of some P-T-X (Fe-Mg) Phase Relations. Am.J.Sci., 276, pp.425-454.

Turner, F.J. and Verhoogen, J. (1960). Igneous and Metamorphic Petrology. McGraw-Hill, New York, 694pp.

Walker, K.R., Joplin, G.A., Lovering, J.F. and Green, R. (1960) Metamorphic and metasomatic convergence of basic igneous rocks and lime magnesia sediments of the Precambrian of north-western Queensland. J.Geol.Soc. Aust. 6, pp.149-178.

Wilson, G. (1984) Structure and Metamorphism of the Tommy Creek Area and a Geochemical Study of the Tommy Creek Microgranite, B.Sc. (Hons.) Thesis University of Adelaide (unpublished).

Wilson, I.H. (1978) Volcanism on a Proterozoic continental margin in north-western Queensland. Prec.Res., 7, pp.205-235.

Winkler, H.J.F. (1979) Petrogenesis of Metamorphic Rocks. 5th Ed. Springer, Verlag, New York, 334pp.

Zakrutkin, V.V. (1968) The evolution of amphiboles during metamorphism. Zap. Uses. Mineral. Obsch., 96, pp.13-23.

APPENDIX I

Thin Section Descriptions

Hand specimen and thin section descriptions of the dominant lithological units are described in detail. Mineral compositions where available are given and were determined by microprobe analysis. Visual estimates of mineral proportions in volume percent are given in table form. A locality map of analysed samples is given at the rear of this appendix.

Mitakoodi Quartzite

Sample	114
Quartz	40
Plagioclase	25
Microcline	25
Calcite	3
Sericite	5
Opaques	2

Sample 830/114

Hand Specimen

A fine grained, cream coloured, inequigranular massive quartzite with porphyroblasts of limonite.

Thin Section

Fine grained, equigranular, granoblastic feldspathic quartzite with calcite porphyroblasts surrounded by hematite.

Plagioclase (0.05-0.1mm) shows distinct twins, generally equigranular anhedral with minor inclusions of sericite. Microcline has a similar habit with distinctive cross hatch twinning. Calcite porphyroblasts (< 3mm) appear to be an alteration product of siderite and are poikiloblastic with inclusions of microcline, plagioclase and quartz. Sericite is present as interstitial grains between feldspars with calcite.

Metabasalt

Sample	35
Quartz	2
Plagioclase	40
Biotite	25
Muscovite	10
Chlorite	10
Epidote	2
Calcite	4
Opaques	7

Sample 830/35

Hand Specimen

A grey-green, massive, fine grained amygdaloidal metabasalt, with vesicles infilled with chlorite and quartz.

Thin Section

Fine grained, equigranular metabasalt with sub-ophitic textures and weak preferred mineral orientation.

Khaki green to pale straw yellow pleochroic biotite (Mg_{50}) shows a weak preferred orientation. Rare masses of biotite define pseudomorphs of igneous phenocrysts.

Plagioclase (< 1.2 mm) is abundant as subhedral laths of random orientation, typical of basaltic textures. Plagioclase composition is Ab_{97} and grain boundaries are cuspate. Inclusions are of predominantly biotite. Chlorite can be found in pods (2-4mm) associated with plagioclase laths.

Scapolitic metasiltstones and calcareous granofels

Sample	I.2	I.3	8	24	157
Quartz	-	5	10	5	5
Tremolite	10	-	-	-	5
Albite	-	10	25	-	15
Orthoclase	-	20	15	10	-
Epidote	-	-	-	10	-
Scapolite	-	5	5	45	-
biotite	15	25	15	15	15
Chlorite	-	-	10	5	-
Calcite	60	35	5	-	55
Sericite	-	-	5	-	-
Magnetite	-	-	5	5	-
Iron Oxide	15	-	-	5	-

Sample 830/24

Hand Specimen

A dark, massive, fine grained metasiltstone with porphyroblasts of scapolite, most evident on weathered surfaces.

Thin Section

Scapolite (mizzonite end member) makes up the bulk of the rock as poikiloblastic porphyroblasts with inclusions of biotite, epidote, magnetite and quartz. Maximum grainsize is 5mm with grains possessing anhedral equant boundaries.

Biotite (0.05-0.1mm) is most abundant between neighbouring scapolite grains, being subhedral equant with a decussate habit.

In the matrix with biotite anhedral poikiloblastic epidote grains (0.05 - .1mm) are common, with inclusions of albite. Minor chlorite in the matrix appears to be exsolving from muscovite.

Quartz is present in a fine grained (0.05 - 0.1mm) groundmass as equant anhedral grains with symmetrical or slight undulose extinction. Grain boundaries are straight to curved, and minor inclusions of iron oxides are present.

Plagioclase occurs as anhedral grains with curved boundaries, and the development of polygonal granoblastic triple joint junctions. Grainsize is similar to quartz in the groundmass, inclusions are predominantly biotite.

Microcline (Ab_5 Or_{95}) shows typical cross hatched twinning and is present in the groundmass as well as anhedral phenocrysts (0.4 - 0.5mm) with slightly kinked twins. Boundaries are lobate or cuspate but show no grain boundary refinement. Minor inclusions within the phenocrysts are biotite and muscovite.

Biotite (Mg_{30}) occurs as small (< 0.15mm) subhedral to anhedral grains showing straw yellow to light brown pleochroism. Muscovite is commonly associated with biotite and may be intergrown. Biotite shows a weak preferred orientation defining the S_1 foliation.

Sample 830/157

Hand Specimen

A massive, finely banded, dark calcareous granofels with fine flecks of actinolite.

Thin Section

Granoblastic, inequigranular, fine grained (0.02-0.1mm) impure limestone.

The matrix consists of fine (< 0.05mm) calcite, pervading the entire rock as equigranular, anhedral, equant grains with minor inclusions of opaques.

Equant grains of quartz of larger grainsize are scattered throughout. The rounded habit of quartz may be the original pre-metamorphic form; they are undeformed but show angular anhedral grain shape.

Albite contains minor inclusions of sericite and are untwinned. Phlogopite with straw yellow to yellow brown pleochroism are equant to elongate with inclusions of calcite and show a weak preferential orientation. Closely associated with biotite are fine needles of actinolite.

Interstitial iron oxides are present throughout the calcite groundmass but not present in quartz and plagioclase.

Biotite-muscovite schist

Sample	52	88	111
Quartz	5	5	25
Plagioclase	-	-	25
Microcline	45	30	2
Garnet	20	-	15
Calcite	-	-	3
Biotite	20	-	30
Muscovite	10	20	-
Ilmenite	-	-	2
Graphite	-	45	-

Sample 830/52

Hand Specimen

A coarse, porphyritic schist containing large, pink garnet porphyroblasts with a crenulated S_2 foliation defined by biotite and muscovite.

Thin Section

Anhedral, elongate garnet porphyroblasts up to 4mm that show zoning, with poikiloblastic cores and inclusion free rims which show renewed growth during S_2. Inclusions in cores are generally parallel to original foliation direction and consist of quartz and feldspar.

Microcline porphyroblasts (2mm) are poikiloblastic and contain curved inclusion trails, with the inclusions at the rims parallel to S_2 foliation.

Biotite occurs as medium grained, interleaved sheaves of yellow to chocolate brown pleochroic subhedral grains defining a strong crenulated cleavage trace. The foliation is cross cut by subhedral fine grained muscovite. Biotite wraps around porphyroblasts of garnet.

Fine grained quartz in the groundmass is equigranular, anhedral and generally coarser grained in garnet inclusions. Grains are composite aggregates with lobate grain boundaries.

Calc-silicate and calc-biotite granofels

Sample	65	105	108
Quartz	-	-	30
Hornblende	-	5	-
Actinolite	25	-	-
Plagioclase	20	15	-
Microcline	-	5	-
Diopside	-	40	-
Garnet	-	-	-
Calcite	50	5	35
Biotite	-	-	5
Chlorite	-	3	20
Epidote	-	5	-
Zoisite	-	15	-
Magnetite	2	-	5
Sphene	2	7	5
Apatite	1	-	-

Sample 830/105

Hand Specimen

Massive, granoblastic, coarse (3-7mm) grained equigranular granofels showing a weak L_2 lineation. Felsic minerals are mainly sericitized plagioclase.

Thin Section

Large, anhedral, elongate to equant diopside make up the majority of the mafic mineralogy, with composition (Ca_{50} Mg_{36} Fe_{14}). Grains (.05-4mm) are highly fractured with inclusions of sphene, hornblende and calcite. Minor hornblende (Ca_{30} Mg_{35} Fe_{35}) occurs as inclusions in diopside but may also be rimming diopside so no correct timing of formation can be ascertained. Hornblende is often rimmed by thin boundaries of tremolite, shows blue green to khaki green pleochroism and characteristic 120° cleavage.

Epidote have variable grainsize and are found as fine enhedral grains in the groundmass (0.1 - 0.5mm) or rare subhedral elongate grains up to 1mm.

Zoisite is common in the groundmass with sericite and appears to be a retrograde product of the breakdown of Ca plagioclase and occurs as fine, subhedral, ragged laths with decussate habit. Albite with lobate boundaries in the groundmass (< .05mm) is clouded by fine hematitic "dust" and often sericitized, and is also associated with Orthoclase and chlorite. Euhedral, brown sphene up to 1.5mm is present as inclusions in diopside.

Amphibolite

Sample	84	91	109_B	147	151
Quartz	-	-	2	-	5
Hornblende	45	45	50	65	55
Microcline	-	50	-	-	-
Plagioclase	-	-	15	20	-
Garnet	-	-	25	-	15
Calcite	2	-	-	3	-
Clinozoisite	15	-	trace	5	3
Epidote	-	5	-	-	1
Sericite	34	4	3	5	20
Ilmenite	4	-	5	2	-
Sphene	-	1	-	-	2

Sample 830/84

Hand Specimen

A foliated fine grained, dark green hornblende rich amphibolite with fractures infilled with quartz.

Thin Section

Euhedral to subhedral hornblende with nematoblastic texture defines an S_1 foliation.

Interlocking grains are common with inclusions of ilmenite and clinozoisite. Prismatic grains up to 5mm show green yellow to light green pleochroism.

Clinozoisite forms in fractures with calcite and quartz and by the alteration of hornblende. Plagioclase is completely sericitized and is associated with fine grained (0.1 - 0.5mm) hornblende and fibrous laths of clinozoisite.

Sample /151

Hand Specimen

A strongly lineated mafic rich rock with porphyroblasts of garnet and quartz. Lineation is defined by hornblendes parallel to the S_1 foliation.

Thin Section

Quartz is present as porphyroblasts (0.5 - 1.5cm) within the pressure shadows of the garnets, which are elongated parallel to the S_2 foliation. Garnet porphyroblasts (20mm) are poikiloblastic with inclusions of plagioclase, clinozoisite and quartz and are elongate parallel to the S_2 foliation. Garnet grains (Ca_{34} Mn_{14} Fe_{52}) are anhedral with strongly lobate boundaries and tend to be fractured.

Hornblende (Ca_{33} Mg_{20} Fe_{47}) occurs as subhedral elongate fine grained (< .8mm) crystals parallel to the foliation direction and show blue green to deep blue green pleochroism. Contacts are often serrated and grains have inclusions of ilmenite and sericitized plagioclase. Minor sphene, calcite and epidote (< .05mm) are present in the groundmass.

Sample 830/57

Hand Specimen

A banded, porphyroblastic, heterogeneous granofels with xenoblastic mineral development. Foliation is defined by preferential orientation of hornblendes.

Thin Section

Inequigranular, weakly foliated with porphyroblasts of garnet and hornblende in a fine (.05 - 1.5mm) granoblastic groundmass.

Garnet (mn_4 Fe_{64} Ca_{32}) is commonly poikiloblastic up to 10mm with inclusions of biotite, calcite, quartz and sphene. The L_1 lineation is continuous through the grains with weak banding continuous through the garnets defined by the abundance of inclusions.

Hornblende (Ca_{31} Mg_{15} Fe_{54}) is also poikiloblastic with anhedral porphyroblasts up to 12mm long, containing inclusions of plagioclase and biotite. Pleochroism is typically khaki green to blue green and grain boundaries are curved, with rare triple point junctions.

Biotite (Mg_{26-28}) is generally fine grained (0.05 - 0.1mm) with red brown to light tan pleochroism and a subhedral to anhedral elongate form parallel to L_2 lineation.

Plagioclase (An_{33}) occurs within the groundmass with biotite and calcite. Twinning is diffuse to distinct in anhedral equant grains with straight grain boundaries and rare triple point boundaries.

Porphyroblasts of quartz (1.0 - 1.6mm) generally as composite aggregates, have lobate boundaries and are closely associated with garnets, being coarsest in the pressure shadows.

Calcite and microcline are minor constituents in the matrix, with calcite also present as medium (0.5 - 1.5mm) undeformed grains in garnets.

	Metadolerite					
Sample	1	7	21	63	64	78
Hornblende	-	-	-	45	50	-
Tremolite	50	45	35	-	-	40
Plagioclase	40	40	40	25	-	55
Epidote	2	-	-	15	45	-
Biotite	-	5	-	10	-	-
Chlorite	3	-	18	-	-	-
Muscovite	-	-	2	-	-	-
Clinozoisite	-	-	2	-	-	-
Ilmenite	5	7	5	5	5	5
Sphene	-	3	3	-	-	-

Sample 830/63

Hand Specimen

Fine grained (< 1mm), homogeneous dolerite with laths of plagioclase in a predominantly felsic groundmass.

Thin Section

Equigranular, holocrystalline, fine grained metadolerite with sub-ophitic textures.

Plagioclase has a decussate habit occurring as subhedral laths (< 0.3mm) with lobate grain boundaries. Grains have diffuse twinning and are weakly undulose. Retrograde metamorphic reactions resulted in the development of epidote as inclusions.

Epidote is closely associated with plagioclase often surrounding plagioclase laths. The grains are equant or fibrous, rarely radiating aggregates with weak green pleochroism and high birefringence. Grain boundaries are cuspate and may show the development of fine grained aggregates.

Hornblende shows blue green to straw yellow pleochroism in xenoblastic elongate grains with ragged boundaries. Biotite can be seen replacing hornblende and grains are generally anhedral equant or elongate.

Sample 830/64

Hand Specimen

Medium grained (2-5mm) massive crystalline metadolerite with porphyroblasts of hornblende and interstitial epidote.

Thin Section

A medium grained bimineralic porphyroblastic metadolerite.

Hornblende (Ca_{29-30} M_{933-46} Fe_{24-37}) shows blue green to green pleochroism and are predominantly equant anhedral to subhedral porphyroblasts, with grain shapes suggesting pyroxene pseudomorphs.

Surrounding the hornblende porphyroblasts in the groundmass are xenoblastic, inequigranular epidote aggregates and are probably forming at the expense of Ca plagioclase.

Tommy Creek Microgranite

Sample	54
Quartz	30
Plagioclase	15
Microcline	45
Biotite	7
Muscovite	3
Zircon	trace

Sample 830/54

Hand Specimen

Light grey massive crystalline rock with gneissic texture and a lineation defined by tabular biotite up to 7mm.

Thin Section

The granite is a fine grained, inequigranular homogeneous rock with porphyritic texture.

Rhyolite

Sample	106
Quartz	48
Plagioclase	30
Hornblende	15
Clinozoisite	2
Muscovite	trace
Ilmenite	3
Sphene	2

Sample 830/106

Hand Specimen

Fine grained, porphyritic rhyolite, essentially undeformed. Phenocrysts up to 4mm of pink plagioclase is a very fine grained groundmass.

Thin Section

Texturally the rhyolite is holocrystalline, massive with phenocrysts in a fine grained matrix. Plagioclase phenocrysts up to 4mm show slightly kinked multiple twins and no preferred orientation. Grain boundaries are commonly embayed with partial grain refinement at the boundaries into small aggregates. Prismatic grain shape is preserved, fractures present are infilled with quartz. Inclusions include hornblende and quartz.

Hornblende occurs as porphyroblasts up to 2mm and are subhedral prismatic, while in the groundmass anhedral grains are generally < 0.05mm. Hornblende shows strong blue-green to straw yellow pleochroism and contains small inclusions of quartz. Elongate grains show a preferred orientation which is related to magmatic flow and not metamorphism.

Quartz shows a weak foliation direction due to magmatic flow also. Grains are generally anhedral equant (< 0.2mm) with slight undulose extinction. Ilmenite occurs as equant grains commonly showing a skeletal structure rimmed by sphene.

SAMPLE LOCALITY

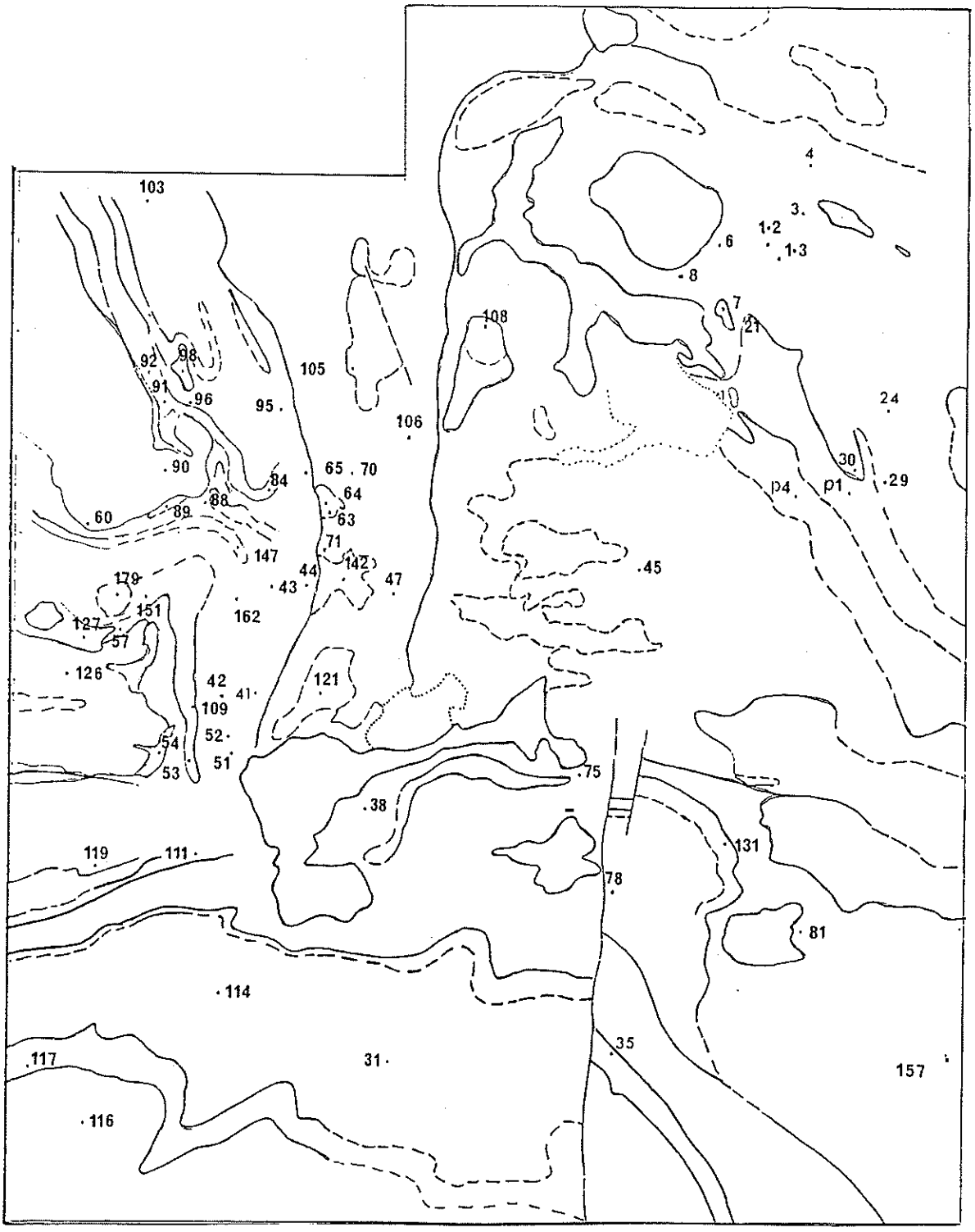

P.N. 1984

APPENDIX II

Analytical Techniques

A. Preparation of Samples

For chemical analysis the samples were prepared by the following methods:-

1) The weathered surfaces were removed and the samples were initially crushed using a jaw crusher.

2) The crushed samples were then ground to a fine powder in a tungsten carbide mill.

3) Approximately 3 gms of powdered sample was then ignited at 960°C to determine the percentage weight loss of volatiles.

4) Approximately 280 mg of the ignited powder was then mixed with 1.5 gms of lithium tetraborate flux and 20 mg of sodium nitrate and fused into buttons for whole rock analysis.

B. Analytical Methods

1) SiO_2, Al_2O_3, Fe_2O_3, MnO, MgO, CaO, K_2O, TiO_2 and P_2O_5 weight percentages were determined on the programmable Siemens XRF machine.

2) Na_2O was determined using the Varian Techtron Atomic Absorption Spectrophotometer. Preparation consisted of digesting approximately 30 mg of ignited sample in a teflon beaker with 10 ml of hydroflouric acid (50%) and 2 ml sulphuric acid for approximately 16 hours. Each solution was diluted to 100 ml and concentration of Na was determined on the spectrophotometer with reference to known standards.

GEOCHEMICAL ANALYSIS OF MAJOR OXIDES

MITAKOODI QUARTZITE

MAJOR ELEMENTS (WEIGHT PERCENT)

	830/114	830/116	830/126	830/131
SiO_2	69.65	89.81	80.54	61.96
Al_2O_3	13.83	3.95	14.58	19.33
Fe_2O_3	3.58	3.67	0.19	8.47
MnO	0.07	0.00	0.00	0.02
MgO	0.61	0.16	0.00	1.12
CaO	2.69	0.03	0.02	0.25
Na_2O	2.21	0.03	0.09	0.28
K_2O	5.78	1.30	4.35	6.45
TiO_2	0.49	0.06	0.08	0.97
P_2O_5	0.20	0.03	0.01	0.20
H_2O	3.07	0.77	3.65	2.71
Total	99.11	98.98	99.86	99.05

OVERHANG JASPILITE

MAJOR ELEMENTS (WEIGHT PERCENT)

	830/6	830/29	830/31	830/38	830/75	830/155
SiO_2	60.45	97.13	60.52	56.38	51.27	7.43
Al_2O_3	20.23	0.08	19.18	6.15	10.65	0.98
Fe_2O_3	7.17	2.18	6.03	22.46	23.11	4.60
MnO	0.05	0.10	0.12	0.89	0.14	2.36
MgO	2.38	0.04	1.84	1.62	2.65	2.27
CaO	0.22	0.13	2.48	6.42	0.32	81.20
Na_2O	0.16	0.02	0.87	0.04	0.06	0.01
K_2O	7.68	0.01	7.18	3.61	4.56	0.26
TiO_2	0.78	0.00	0.75	0.25	0.41	0.04
P_2O_5	0.15	0.08	0.23	0.19	0.21	0.19
H_2O	3.49	0.27	4.31	8.91	3.12	8.11
Total	99.28	99.27	99.19	98.02	99.38	99.35

	830/183A	830/184	830/P4
SiO_2	70.93	41.15	59.76
Al_2O_3	12.51	4.42	12.16
Fe_2O_3	7.00	4.08	7.91
MnO	0.21	3.93	0.15
MgO	2.46	17.75	2.00
CaO	0.17	25.13	8.24
Na_2O	0.08	0.02	1.72
K_2O	5.06	1.76	6.39
TiO_2	0.53	0.19	0.59
P_2O_5	0.14	0.17	0.22
H_2O	1.98		5.64
Total	99.10	98.59	99.14

CORELLA CALC-SILICATES

MAJOR ELEMENTS (WEIGHT PERCENTAGE)

	830/43	830/44	830/51	830/60	830/91	830/96
SiO_2	56.36	71.94	32.86	52.77	52.91	52.05
Al_2O_3	12.85	12.98	7.30	14.80	16.19	13.70
Fe_2O_3	5.07	4.32	24.38	10.62	8.01	8.92
MnO	0.08	0.04	0.92	0.39	0.23	0.53
MgO	4.57	0.75	7.21	5.08	5.23	4.98
CaO	13.78	0.59	23.87	8.00	8.58	10.68
Na_2O	5.43	4.09	0.73	3.06	0.60	1.60
K_2O	0.55	4.11	0.30	4.31	7.24	5.58
TiO_2	0.48	0.55	1.07	0.65	0.66	0.90
P_2O_5	0.14	0.11	0.30	0.15	0.19	0.24
H_2O	11.07	0.72	13.24	2.30	1.60	3.09
Total	99.30	99.47	98.94	99.81	99.78	99.19

	830/103	830/105
SiO_2	52.47	52.17
Al_2O_3	14.77	13.94
Fe_2O_3	9.25	5.78
MnO	0.19	0.16
MgO	6.55	5.52
CaO	7.70	17.13
Na_2O	2.91	2.75
K_2O	4.70	1.19
TiO_2	0.58	1.36
P_2O_5	0.21	0.15
H_2O	3.26	2.74
Total	99.31	100.15

CORELLA QUARTZITES
MAJOR ELEMENTS (WEIGHT PERCENTAGE)

	830/42	830/95	830/98	830/162
SiO_2	71.94	79.58	68.36	82.09
Al_2O_3	12.26	9.40	13.58	9.62
Fe_2O_3	2.85	1.71	6.52	0.29
MnO	0.06	0.01	0.24	0.01
MgO	0.41	0.00	0.33	0.09
CaO	3.76	0.05	0.05	0.10
Na_2O	5.88	0.23	0.31	0.88
K_2O	0.70	7.81	9.84	6.07
TiO_2	0.26	0.40	0.56	0.11
P_2O_5	0.02	0.05	0.04	0.06
H_2O	3.08	1.27	0.85	1.09
Total	98.14	99.24	99.83	99.32

CORELLA BIOTITE - MUSCOVITE SCHIST
MAJOR ELEMENTS (WEIGHT PERCENTAGE)

	830/52	830/88	830/92	830/183B
SiO_2	63.83	73.36	56.88	77.82
Al_2O_3	14.21	18.15	14.25	14.74
Fe_2O_3	13.90	0.67	7.56	0.91
MnO	0.36	0.00	0.04	0.00
MgO	0.93	0.61	8.63	0.42
CaO	0.41	0.11	0.40	0.05
Na_2O	0.10	0.40	5.85	0.23
K_2O	4.76	5.14	4.37	4.46
TiO_2	0.95	0.75	0.54	0.73
P_2O_5	0.18	0.22	0.33	0.08
H_2O	1.83	9.09	12.82	8.50
Total	99.57	99.35	98.85	99.45

AMPHIBOLITES

MAJOR ELEMENTS (WEIGHT PERCENTAGE)

	830/109	830/121	830/127	830/147	830/151
SiO_2	45.75	50.81	48.25	45.77	46.89
Al_2O_3	14.01	12.17	15.65	16.78	20.73
Fe_2O_3	22.57	16.38	12.93	13.92	13.89
MnO	0.50	0.13	0.22	0.26	0.89
MgO	3.39	5.05	6.12	6.71	2.80
CaO	7.67	6.25	11.61	11.07	14.39
Na_2O	0.63	2.88	2.58	2.26	1.02
K_2O	0.73	2.33	0.23	0.79	1.89
TiO_2	3.37	2.88	1.53	1.91	2.87
P_2O_5	0.37	0.30	0.30	0.23	0.33
H_2O	0.14	3.57	1.46	1.01	2.55
Total	98.99	99.17	99.43	99.71	99.70

META-DOLERITES

MAJOR ELEMENTS (WEIGHT PERCENTAGE)

	830/1	830/7	830/45	830/47	830/84	830/117
SiO_2	49.82	48.53	48.87	51.49	47.02	52.75
Al_2O_3	14.41	12.58	14.98	14.96	16.74	14.36
Fe_2O_3	13.73	17.62	12.77	11.89	13.73	16.73
MnO	0.18	0.18	0.18	0.17	0.27	0.12
MgO	7.76	5.12	7.89	5.85	6.78	6.42
CaO	8.30	7.59	9.28	7.70	9.19	1.87
Na_2O	3.69	3.46	3.03	3.41	2.56	3.67
K_2O	0.21	1.15	1.41	2.63	1.58	0.89
TiO_2	1.22	2.79	0.89	1.23	1.72	2.30
P_2O_5	0.09	0.38	0.07	0.12	0.23	0.27
H_2O	0.70	0.84	1.12	1.07	1.85	3.32
Total	99.4	99.40	99.37	99.39	99.82	99.38

	830/142	830/P1
SiO_2	56.20	50.92
Al_2O_3	12.23	14.39
Fe_2O_3	13.25	12.46
MnO	0.44	0.22
MgO	1.76	6.62
CaO	6.85	10.23
Na_2O	3.52	2.91
K_2O	1.46	0.79
TiO_2	2.06	1.08
P_2O_5	0.54	0.10
H_2O	2.70	1.08
Total	98.30	99.72

TOMMY CREEK MICROGRANITE

NARAKU GRANITE

MAJOR ELEMENTS (WEIGHT PERCENTAGE)

	830/54	830/70	830/71	830/90	830/179	830/126
SiO_2	75.85	75.87	72.38	74.71	76.66	80.54
Al_2O_3	11.80	13.56	13.29	13.32	14.52	14.58
Fe_2O_3	3.37	0.27	4.21	1.10	0.24	0.19
MnO	0.05	0.01	0.03	0.05	0.01	0.00
MgO	0.48	0.25	1.79	0.40	0.21	0.0
CaO	0.04	1.48	0.42	1.40	0.37	0.02
Na_2O	0.30	6.68	4.26	3.93	7.07	0.09
K_2O	7.85	0.18	2.36	4.57	0.50	4.35
TiO_2	0.12	0.57	0.49	0.38	0.43	0.08
P_2O_5	0.02	0.17	0.09	0.06	0.04	0.01
H_2O	0.89	0.54	1.48	1.01	0.77	3.65
Total	99.87	99.05	99.32	99.92	100.04	99.86

APPENDIX III

Electron Microprobe Analysis of Mineral Compositions

The electron microprobe analyses were obtained on the Joel Electron Microprobe using carbon coated polished thin sections.

Samples	
830/1	Meta-dolerite
830/3	Meta-dolerite
830/4	Meta-dolerite
830/24	Scapolitic meta-siltstone
830/30	Scapolitic meta-siltstone
830/35	Meta-basalt
830/41	Calc-silicate granofels
830/52	Garnet-biotite schist
830/53	Amphibolite
830/54	Microgranitic gneiss
830/57	Amphibolite
830/64	Amphibolite
830/65	Calc-silicate granofels
830/81	Garnet-biotite meta-siltstone
830/89	Hematitic siltstone
830/96	Calc-silicate granofels
830/105	Calc-silicate granofels
830/109B	Garnet-hornblende amphibolite
830/111	Garnet-biotite schist
830/119	Garnet-biotite schist
830/147	Amphibolite
830/151	Garnet-hornblende amphibolite

GARNET

GARNET-BIOTITE SCHISTS | AMPHIBOLITE

Sample 830/	052-1	052-2	111	119	109_B	151
SiO_2	39.39	37.10	36.99	37.5	37.57	37.34
TiO_2	0.71	-	0.15	0.12	-	0.22
Al_2O_3	20.36	21.36	20.74	20.46	21.39	26.68
FeO	31.24	35.01	26.97	22.64	29.90	20.64
MnO	2.01	2.68	3.73	8.03	0.97	5.29
MgO	0.52	0.85	0.59	0.80	1.59	1.79
CaO	4.19	3.59	10.23	11.07	8.72	13.07
Na_2O	-	0.17	-	-	-	-
Cr_2O_3	0.13	-	-	-	-	-
Total	99.53	100.76	99.39	100.03	100.13	99.04

STRUCTURAL FORMULAE (BASED ON 12 OXYGENS PER FORMULA UNIT)

Si	3.1526	2.9924	2.9904	3.0080	2.9957	2.9870
Ti	0.0425	-	0.0094	0.0073	-	0.0135
Al	1.9211	2.0300	1.9761	1.9330	2.0101	1.9503
Fe	2.0911	2.3615	1.8233	1.4777	1.9938	1.3812
Mn	0.2038	0.1828	0.2552	0.5452	0.0652	0.3582
Mg	0.0617	0.1025	0.0712	0.0959	0.1890	0.2136
Ca	0.3589	0.3104	0.8864	0.9511	0.7454	1.1206
Na	-	0.0260	-	-	-	-
Total	7.8401	8.0055	8.0120	8.0182	7.9991	8.0425

PLAGIOCLASE

	AMPHIBOLITES			METABASALT	
Sample 830/	053-1	053-2	053-3	147	035
SiO_2	70.00	64.58	64.95	63.56	69.92
Al_2O_3	20.48	23.35	22.4	21.90	20.02
FeO	-	0.57	0.36	-	0.21
MgO	-	0.29	0.14	-	-
CaO	0.66	0.62	12.34	3.00	0.35
Na_2O	8.61	5.37	8.97	9.15	9.06
K_2O	-	2.30	0.66	-	0.08
Cl	0.12	-	0.10	-	0.04
Total	99.87	97.08	99.92	97.62	99.68

STRUCTURAL FORMULAE (BASED ON 32 OXYGENS PER FORMULA UNIT)

Si	12.0916	11.5648	11.4416	11.4316	12.1188
Al	4.1688	4.9288	4.6512	4.6400	4.0904
Fe	-	0.0856	0.0536	-	0.0296
Mg	-	0.0784	0.0372	-	-
Ca	0.1216	0.1192	0.1105	0.5776	0.0652
Na	2.8830	1.8628	3.0648	3.1904	3.0464
K	-	0.5248	0.148	-	0.0172
Total	19.3024	19.1644	19.8692	19.8424	19.3676

PLAGIOCLASE

	METADOLERITES			GARNET-BIOTITE SCHIST	
Sample 830/	001	003	004	111	119
SiO_2	63.45	68.92	70.33	61.22	65.38
Al_2O_3	24.33	20.32	20.02	24.11	22.36
FeO	-	0.28	0.20	0.33	0.14
CaO	5.37	0.35	0.09	5.37	2.98
Na_2O	7.69	11.06	9.90	7.51	9.35
K_2O	0.07	0.07	0.07	0.22	0.15
Cl	-	-	-	0.07	-
Total	100.90	100.99	100.61	99.00	100.45

STRUCTURAL FORMULAE (BASED ON 32 OXYGENS PER FORMULA UNIT)

Si	11.0860	11.9128	12.102	10.958	11.4308
Al	5.0088	4.1388	4.0612	5.0876	4.5944
Fe	-	0.0412	0.0284	0.0492	0.0208
Ca	1.0048	0.0652	0.0168	1.0300	0.5580
K	0.0152	0.0148	0.0148	0.0512	0.0152
Na	2.6048	3.7048	3.3028	2.6072	3.1684
Total	19.7196	19.8776	19.5264	19.8492	19.826

PLAGIOCLASE

CALC-SILICATES

Sample 830/	057	065	096	105
SiO_2	60.78	68.01	69.46	69.41
Al_2O_3	25.83	19.74	19.81	19.93
FeO	0.16	0.29	-	-
CaO	6.77	0.35	0.11	0.09
Na_2O	7.61	11.07	11.04	11.13
K_2O	0.07	-	0.10	-
Cl	0.06	0.06	-	-
Total	101.28	99.53	100.53	100.57

STRUCTURAL FORMULAE (BASED ON 32 OXYGENS PER FORMULA UNIT)

Si	10.6848	12.1664	12.0252	12.0092
Al	5.3512	4.0164	4.0428	4.0648
Fe	0.0228	0.0421	-	-
Ca	1.2748	0.0128	0.0053	1.0172
K	0.0040	0.024	0.0057	-
Na	2.5944	3.0556	3.706	3.7336
Total	19.9608	19.302	19.818	19.8252

AMPHIBOLE

AMPHIBOLITES

Sample 830/	053	109_B	147-1	147-2	151	064-1
SiO_2	45.85	39.57	43.86	50.97	40.40	54.63
TiO_2	0.69	0.58	0.83	-	0.70	-
Al_2O_3	10.26	16.38	12.50	0.85	13.85	0.58
FeO	18.22	20.72	16.57	23.24	21.43	13.33
MnO	0.24	-	0.20	0.24	0.26	0.13
MgO	9.65	5.72	9.35	7.55	5.03	15.04
CaO	11.70	11.16	11.89	12.22	11.52	12.34
Na_2O	1.10	1.22	1.04	-	0.51	-
K_2O	0.46	1.06	0.38	-	1.25	-
Cl	0.37	0.39	0.13	-	0.21	-
Total	98.90	96.74	96.74	95.07	95.19	96.04

STRUCTURAL FORMULAE (BASED ON 23 OXYGENS PER FORMULA UNIT)

Si	6.8017	6.1259	6.5924	7.9516	6.9466	7.9942
Ti	0.0770	0.0670	0.0939	-	0.0835	-
Al	1.7944	2.9881	2.2148	0.1557	2.5776	0.0995
Fe	2.2606	2.6825	2.0825	3.034	2.8305	1.6312
Mn	0.0301	-	0.0255	0.0313	-	0.0158
Mg	2.1347	1.3199	2.0937	1.7555	1.1846	3.2801
Ca	1.860	1.8412	1.9148	2.0422	2.0382	1.9352
K	0.0864	0.2089	0.0727	-	0.2509	-
Na	0.3159	0.3670	0.3038	-	0.1569	-
Cl	0.0922	0.1017	0.0324	-	0.0572	-
Total	15.4959	15.7024	15.4267	14.9705	15.5088	14.9560

AMPHIBOLE

	AMPHIBOLITES			META-DOLERITES	
Sample 830/	64-2	1-1	1-2	3	4
SiO_2	42.60	46.08	51.74	55.34	51.57
TiO_2	0.19	0.25	0.19	-	0.16
Al_2O_3	11.52	10.42	5.39	2.52	5.16
FeO	17.99	13.94	10.65	9.17	11.46
MnO	0.50	0.18	0.16	-	-
MgO	9.02	12.21	15.98	18.55	16.01
CaO	11.42	11.63	12.09	12.14	11.94
Na_2O	1.24	1.24	0.51	0.52	0.89
K_2O	0.25	0.09	-	-	-
Total	94.75	96.02	96.71	98.22	97.44

STRUCTURAL FORMULAE (BASED ON 23 OXYGENS PER FORMULA UNIT)

Si	6.6036	6.8522	7.4563	7.7631	6.7937
Ti	0.0227	0.0274	0.0069	-	0.0162
Al	2.1039	1.8257	0.9145	0.4160	8.8012
Fe	2.3325	1.7335	1.2831	1.1226	1.2625
Mn	0.0661	0.0228	0.0198	-	-
Mg	2.0844	2.7059	3.4328	3.8795	3.2862
Ca	1.8972	1.8526	1.8667	1.8240	1.6851
Na	0.3732	0.3577	0.1428	0.1407	0.2262
K	0.0489	0.0169	-	-	-
Total	15.5328	15.3947	15.1369	15.0993	13.9706

AMPHIBOLE

CALC-SILICATES

Sample 830/	65	96	105
SiO_2	54.53	54.15	44.54
TiO_2	-	-	0.47
Al_2O_3	1.52	1.89	9.77
FeO	9.22	11.74	18.02
MnO	-	1.28	-
MgO	18.23	16.16	10.05
CaO	11.35	11.88	11.77
Na_2O	0.38	0.21	1.32
K_2O	0.10	0.09	0.71
Cl	0.05	0.07	0.58
Total	95.39	97.47	97.42

STRUCTURAL FORMULAE (BASED ON 23 OXYGENS PER FORMULA UNIT)

Si	7.8772	7.8028	6.7540
Ti	-	-	0.0536
Al	0.2586	0.3216	1.7462
Fe	1.1141	1.4144	2.2850
Mn	-	0.1562	-
Mg	3.9245	3.4708	2.2710
Ca	1.7561	1.8334	1.913
Na	0.1067	0.0598	0.389
K	0.0191	0.0168	0.137
Total	15.0688	15.0899	15.7209

BIOTITE

	GARNET-BIOTITE SCHISTS				CALC-SILICATES	META-BASALT
Sample 830/	052	081	111	119	041	035
SiO_2	33.75	33.32	32.56	33.63	41.13	36.57
TiO_2	3.22	1.32	2.62	3.89	1.15	1.71
Al_2O_3	18.78	17.06	16.43	16.92	11.58	16.48
FeO	28.10	25.99	29.95	26.33	9.99	18.12
MnO	-	0.27	0.20	0.54	-	-
MgO	2.73	5.98	2.78	4.13	20.43	11.27
K_2O	9.23	8.80	8.78	9.15	8.85	9.20
Cl	-	0.48	0.83	-	0.16	0.07
Total	96.92	93.14	94.13	94.59	93.29	93.42

STRUCTURAL FORMULAE (BASED ON 23 OXYGENS PER FORMULA UNIT)

Si	5.3416	5.4237	5.3831	5.3809	6.0745	5.6390
Ti	0.3834	0.1615	0.3256	0.4679	0.1274	0.1986
Al	3.5034	3.2734	3.2023	3.1906	2.0167	2.9951
Fe	3.7197	3.5378	4.1408	3.5238	1.2347	2.3365
Mn	-	0.0369	0.0277	-	-	-
Mg	0.6430	1.4306	0.6847	0.0734	4.4990	2.5911
K	1.8638	1.8273	1.8511	0.9853	1.8185	1.8091
Cl	0.2993	0.1334	0.2313	1.8677	0.0399	0.0194
Total	15.7542	15.824	15.8466	15.4895	15.6611	15.5879

BIOTITE

OVERHANG JASPILITE

Sample 830/	016	024	030	089
SiO_2	40.68	36.32	41.25	46.31
TiO_2	0.11	2.02	0.65	-
Al_2O_3	15.68	16.98	16.14	11.00
FeO	11.44	17.18	3.89	13.33
MnO	0.22	-	0.61	-
MgO	13.99	11.81	22.31	18.91
CaO	0.24	-	0.14	-
K_2O	6.89	9.47	8.96	9.08
Cl	0.05	0.26	-	0.12
Total	89.32	94.05	93.95	92.73

STRUCTURAL FORMULAE (BASED ON 22 OXYGENS PER FORMULA UNIT)

Si	6.1926	5.5603	5.8589	6.1081
Ti	0.0128	0.2328	0.0694	-
Al	2.8137	3.0631	2.7014	1.9647
Fe	1.4565	2.1997	0.5886	1.6890
Mn	0.0288	-	0.0939	-
Mg	3.1746	2.6946	4.7225	4.2702
Ca	0.0397	-	0.0211	-
K	1.3378	1.8486	1.6225	1.7552
Cl	0.0128	0.0669	-	0.0298
Total	15.0693	15.6662	15.5321	15.8168

EPIDOTE

Sample 830/	024	064	96	105	109B	151
SiO_2	38.64	38.97	38.04	43.58	37.01	38.95
Al_2O_3	23.42	19.10	21.68	22.50	24.32	28.92
FeO	11.57	13.88	13.87	2.76	6.07	5.34
MnO	0.15	0.25	-	-	-	-
MgO	0.12	2.43	0.24	0.13	2.31	-
CaO	23.09	20.11	23.09	25.81	22.27	23.19
Na_2O	0.20	-	-	-	-	-
K_2O	-	0.09	-	-	-	-
P_2O_5	-	-	-	-	-	0.15
Total	97.18	94.82	96.92	95.02	91.99	96.55

STRUCTURAL FORMULAE (BASED ON 12 OXYGENS PER FORMULA UNIT)

Si	3.0188	3.1438	3.0208	3.3402	2.9725	2.9459
Al	2.1564	1.8157	2.0293	2.0186	2.3026	2.5775
Fe	0.7563	0.9367	0.9212	0.1721	0.4080	0.3379
Mn	0.0097	0.0170	-	-	-	-
Mg	0.0140	0.2917	0.0287	0.0147	0.2776	-
Ca	1.9327	1.7387	1.9645	2.1048	1.9167	1.8796
Na	0.0298	-	-	-	-	-
K	-	0.0092	-	-	-	-
Total	7.9177	7.9528	7.9644	7.6503	7.8763	7.7506

SCAPOLITE

METASILTSTONES

Sample 830/	24	30
SiO_2	49.62	53.25
Al_2O_3	25.75	26.69
CaO	14.44	12.56
K_2O	0.42	0.52
Na_2O	4.20	5.68
Cl	0.98	1.57
SO_3	1.26	-
Total	96.67	100.27

STRUCTURAL FORMULAE (BASED ON 24 OXYGENS PER FORMULA UNIT)

Si	7.1082	7.3881
Al	4.3478	4.3647
Ca	2.2166	1.8669
K	0.0775	0.0921
Na	1.1662	1.5273
Cl	0.2368	0.3693
S	0.1270	-
Total	15.2801	15.6084

APPENDIX IV

Niggli Values

Often used to differentiate ortho and para-amphibolites and are determined by converting element oxide weight percentages to molecular proportions. Niggli al, fm, c and alk are calculated as percentages of the sum of the major cation elements (except SiO_2).

i.e. al = Al_2O_3 as a percentage of Al_2O_3 + FeO + MgO + MnO + CaO + Na_2O + K_2O.

fm = FeO + MgO + MnO

c = CaO

alk = Na_2O + K_2O

where al + fm + c + alk = 100

mg is simply the fraction of MgO in the transition element oxides MgO, FeO and MnO

i.e. $$mg = \frac{MgO}{FeO+MgO+MnO}.$$

ACF values

Element oxide weight percentages are converted to molecular proportions and A, C, F are calculated according to:-

$$A = [Al_2O_3] + [Fe_2O_3] - [Na_2O] - [K_2O]$$
$$C = [CaO] - 3.3[P_2O_5]$$
$$F = [MgO] + [MnO] + [FeO]$$

where A + C + F = 100

NIGGLI VALUES, A.C.F VALUES

OVERHANG JASPILITE

Sample 830/	6	29	31	38	75
al	44.48	2.1	41.43	10.41	19.02
fm	35.78	90.28	28.95	63.09	70.94
c	0.87	6.39	9.70	19.76	1.60
alk	18.86	1.10	19.80	6.73	8.99
mg	0.37	0.03	0.35	0.11	0.17
A	37.02	25.55	56.24	19.98	45.10
C	0.30	1.77	16.92	26.19	0.25
F	62.67	72.68	26.84	53.82	54.65

Sample 830/	155	183A	184	P4
al	0.59	70.86	4.08	22.77
fm	9.49	24.43	51.99	30.90
c	89.74	0.40	42.14	28.05
alk	0.10	7.30	1.78	9.50
mg	0.37	0.38	0.79	0.31
A	1.61	16.01	3.66	19.03
C	91.31	0.00	44.16	49.06
F	7.07	83.98	52.16	31.90

CORELLA CALC-SILICATES

Sample 830/	43	44	51	52	60	91	96
al	19.38	38.95	7.37	33.19	21.96	24.69	33.61
fm	28.47	24.27	54.67	52.80	42.20	38.04	31.93
c	37.78	3.20	43.79	1.70	21.50	23.80	23.82
alk	14.37	33.55	1.54	12.27	14.37	8.65	10.64
mg	0.61	0.24	0.34	0.10	0.45	0.53	0.48
A	13.42	44.51	9.09	43.03	18.91	24.26	17.88
C	56.46	9.71	43.24	1.26	32.34	34.79	40.98
F	30.12	45.78	47.67	55.71	48.74	40.95	41.13

Sample 830/	103	105
al	21.52	19.02
fm	43.69	30.57
c	20.40	42.49
alk	14.39	7.90
mg	0.55	0.62
A	18.20	18.36
C	30.37	52.91
F	51.43	28.73

CORELLA BIOTITE - MUSCOVITE SCHISTS

Sample 830/	52	88	92	183B
al	33.19	67.05	22.99	65.82
fm	52.80	9.22	52.66	10.52
c	1.70	0.70	1.17	0.40
alk	12.27	22.99	23.17	23.25
mg	0.10	0.62	0.67	0.45
A	43.03	82.72	6.01	85.76
C	1.26	0.00	0.00	0.00
F	55.71	17.28	93.98	14.29

AMPHIBOLITES

Sample 830/	109	121	127	147	151
al	19.70	18.16	20.75	21.35	26.34
fm	58.13	54.04	45.30	47.22	35.68
c	19.07	16.96	27.99	25.61	33.24
alk	2.57	10.80	4.40	4.50	4.70
mg	0.21	0.31	0.45	0.46	0.25
A	31.60	19.57	23.22	23.67	33.78
C	22.24	20.81	33.01	30.37	39.92
F	46.16	59.62	34.79	45.96	26.29

META-DOLERITES

Sample 830/	1	7	45	47	84	117	142	P1
al	19.16	17.58	19.64	21.37	21.91	22.11	21.86	19.61
fm	52.39	53.40	50.05	46.08	48.47	61.66	42.71	47.36
c	20.06	19.28	21.84	20.02	21.87	5.24	22.26	25.34
alk	8.39	9.60	8.47	12.21	7.75	10.78	13.18	7.70
mg	0.50	0.34	0.52	0.46	0.46	0.40	0.34	0.48
A	22.11	24.58	19.57	23.42	26.33	22.76	28.24	20.56
C	26.15	26.35	28.03	29.43	28.31	5.95	33.82	31.61
F	51.74	49.07	52.40	47.15	45.36	71.29	37.93	47.83

APPENDIX V

Determination of fluid pressures

The determination of fluid compositions, temperatures and pressures are discussed in detail in Ferry (1976).

The general thermodynamic equation

$$\Delta H - \Delta S\, T + \Delta V_S P + RT \ln K_S + m\, RT \ln f_{CO2} + n\, RT \ln f_{CO2} = 0$$

can be used for stoichiometric relations of minerals in equilibrium.

Notation:-

- P lithostatic pressure (bars)
- T temperature (°K)
- f_i fugacity of component i
- R universal gas constant
- K_S activity constant for an assemblage of solid mineral phases
- ΔV_S differences in molar volumes between solid reactants and solid products (calories/bar)
- ΔH molar enthalpy of reaction (calories)
- ΔS molar entropy (in phase)
- $a_{i,j}$ activity of component i in phase j
- $X_{i,j}$ mole fraction of component i in phase j
- γ_i fugacity coefficient for component i

K_S can be determined from the activities of minerals determined from atomic proportions of elements derived from microprobe analyses.

Calcite : $a_{cc} = X_{Ca,cc}$

Zoisite : $a_{zo} = X^3_{Al,TCS}$

Garnet : $a_{gr} = X^3_{Ca,DCS}$

Diopside : $a_{di} = X_{Ca,M2}\, X_{mg,M1}$ where $X_{Ca,M2}$ = mole fraction of Ca in M_2 site

Muscovite : $a_{mv} = X_{K,A}\, X^2_{Al,M2}$

Biotite : $a_{ph} = X_{KA} X^3_{Mg,M}$

Calcic amphibole : $a_{tr} = [3\text{-}Ca\text{-}Na\text{-}K].[Ca/2]^2.[Mg/5]^5.[OH/2]^2$

ΔH, ΔS ΔV can be obtained for each element from thermodynamic tables of Robie et al. (1978).

Determination of partial pressures (p_i) from fugacities requires the knowledge of fugacity coefficients. Tables of fugacity coefficients γ° are given for the required temperatures and pressures for selected fluids in Ryzhenko et al. (1971).

Assuming

$$P_{fluid} = P_{CO2} + P_{H2O} = P_{total} \quad \text{(Ferry, 1976)}$$

$$= f_{CO2}/\gamma_{CO2} + f_{H2O}/\gamma_{H2O} = P_{total}$$

Mole fractions of CO_2

$$X_{CO2} = f_{CO2}/\gamma_i P$$

APPENDIX VI

Geothermometry

1) Garnet-Biotite Geothermometry

Garnet-biotite geothermometry was undertaken with the aid of a computer program by Fanning, 1980.

Calibration of Fe-Mg distribution between garnet and biotite is expressed as $K_D = (Mg/Fe)_{ga} / (Mg/Fe)_{bi}$. The variation in temperature values is the result of different methods of determining Fe-Mg exchange.

Thompson (1976) calibrated Fe-Mg distribution between garnet and biotite with temperature by using temperatures based upon other phase equilibria.

Goldmann and Albee (1977) correlated K_D with oxygen isotope fractionation in coexisting quartz and iron-titanium oxides.

Ferry and Spear (1978) reported experimental data on Mg-Fe exchange between synthetic garnet and biotite.

Variation in temperatures can be due to the effects of cations other than Fe-MG, i.e. Ti in biotite can significantly displace K_D at constant P and T. Goldmann and Albee made quantitative estimates of the effects of Ca and Mn contents of garent and the Fe, Ti and octahedral Al(Al^{vi}) contents of biotite on the correlations between K_D and the oxygen isotope fractionation constant. The high T obtained from this method suggests other factors affecting K_D are involved.

2) Garnet-Hornblende Geothermometry

The garnet-hornblende Fe-Mg exchange has been calibrated against a garnet-clinopyroxene geothermometer by Graham et al (1984), where

$K_D = (Fe/Mg)_{ga} / (Fe/Mg)_{hb}$ for ideal solid solutions and a geothermometer of the form

$$T(°K) = \frac{2880 + 3280\ X_{Ca,ga}}{\ln K_D + 2.426}$$

provides good agreement between garnet-hornblende and garnet-clinopyroxene temperatures.